Global Ecology and Biogeography, (Global Ecol. Biogeogr.) (2011) **20**, 532–544

A Journal of Macroecology

Global Ecology and Biogeography

RESEARCH PAPER

Geographic disparities and moral hazards in the predicted impacts of climate change on human populations

J. Samson[1]*, D. Berteaux[2], B. J. McGill[3] and M. M. Humphries[1]

[1]*Department of Natural Resource Sciences, Macdonald Campus, McGill University, 21,111 Lakeshore Road, Ste-Anne-de-Bellevue, QC, Canada, H9X 3V9,* [2]*Canada Research Chair in Northern Ecosystem Conservation and Centre d'Études Nordiques, Université du Québec à Rimouski, 300, Allée des Ursulines, Rimouski, QC, Canada, G5L 3A1,* [3]*School of Biology and Ecology Sustainability Solutions Initiative, University of Maine, 5751 Murray Hall, Orono, ME 04469, USA*

*Correspondence: J. Samson, Department of Natural Resource Sciences, Macdonald Campus, McGill University, 21,111 Lakeshore Road, Ste-Anne-de-Bellevue, QC, Canada, H9X 3V9.
E-mail: jason.samson@mail.mcgill.ca

ABSTRACT

Aim It has been qualitatively understood for a long time that climate change will have widely varying effects on human well-being in different regions of the world. The spatial complexities underlying our relationship to climate and the geographical disparities in human demographic change have, however, precluded the development of global indices of the predicted regional impacts of climate change on humans. Humans will be most negatively affected by climate change in regions where populations are strongly dependent on climate and favourable climatic conditions decline. Here we use the relationship between the distribution of human population density and climate as a basis to develop the first global index of predicted impacts of climate change on human populations.

Location Global.

Methods We use spatially explicit models of the present relationship between human population density and climate along with forecasted climate change to predict climate vulnerabilities over the coming decades. We then globally represent regional disparities in human population dynamics estimated with our ecological niche model and with a demographic forecast and contrast these disparities with CO_2 emissions data to quantitatively evaluate the notion of moral hazard in climate change policies.

Results Strongly negative impacts of climate change are predicted in Central America, central South America, the Arabian Peninsula, Southeast Asia and much of Africa. Importantly, the regions of greatest vulnerability are generally distant from the high-latitude regions where the magnitude of climate change will be greatest. Furthermore, populations contributing the most to greenhouse gas emissions on a per capita basis are unlikely to experience the worst impacts of climate change, satisfying the conditions for a moral hazard in climate change policies.

Main conclusions Regionalized analysis of relationships between distribution of human population density and climate provides a novel framework for developing global indices of human vulnerability to climate change. The predicted consequences of climate change on human populations are correlated with the factors causing climate change at the regional level, providing quantitative support for many qualitative statements found in international climate change assessments.

Keywords

Climate change, climate vulnerability, demography, ecological niche model, geographically weighted regression, human populations, moral hazard.

DOI: 10.1111/j.1466-8238.2010.00632.x
© 2011 Blackwell Publishing Ltd http://wileyonlinelibrary.com/journal/geb

INTRODUCTION

Recent international assessments of the societal impacts of climate change have repeatedly stressed the importance of defining regional vulnerabilities to inform adaptation policies (WHO, 2004; Patz *et al.*, 2005; IPCC, 2007; Lobell *et al.*, 2008; World Water Assessment Programme, 2009). The importance of geographic disparities in the impact of current climate variability on human populations has also received much attention, with the 2003 European heat wave (Poumadère *et al.*, 2005; Chase *et al.*, 2006), recent droughts in Australia (Horridge *et al.*, 2005) and California (Service, 2009), and dramatic impacts on the traditional lifestyles of Inuit communities (Ford & Smit, 2004). Furthermore, there is strong evidence that climate change has played a major role in defining the history of human civilizations (Weiss *et al.*, 1993; Kuper & Kropelin, 2006) and widespread scepticism that modern technology and globalization will globally alleviate the negative impacts of climate change (Zhang *et al.*, 2007; Burke *et al.*, 2009; Costello *et al.*, 2009; Trouet *et al.*, 2009). The complexity of regional dynamics underlying the coupled human–environment system has, however, restricted most assessments of climate vulnerability to qualitative or regional approaches (Adger, 2006). Spatial variability in the magnitude and direction of the impacts of climate change makes it challenging but important to develop global indices of regional vulnerability to climate change (Dyson, 2005).

Niche modelling is an increasingly common approach used by ecologists to predict species responses to climate change (Peterson, 2003; Austin, 2007). The approach assumes that a species' response to climate change can be anticipated by modelling how environmental niches currently occupied by the species will contract, expand and/or move as a result of climate change (Austin, 2007). Application of niche modelling to predict the impacts of climate change on human populations is potentially problematic for many reasons, but most of these problems are not unique to humans. The possibility that the current distribution of humans reflects where humans choose to live, not where they are capable of living, that the distribution of humans is dictated more by historical contingencies than current climate conditions, that any apparent relationship between human populations and climate is indirect and likely to be mediated by the distribution of resources, that the current association between humans and climate may not persist in a rapidly changing world, and that humans are too complex to model using simple associations between climate and distribution, are possibilities that also apply, albeit to a lesser degree, to all the non-human organisms that have been studied with ecological niche modelling. As a result, these potential limitations have been widely discussed and debated in the literature on ecological niche modelling in the context of other animals and plants (see reviews by Pearson & Dawson, 2003; Austin, 2007). The application of niche modelling to human populations can thus be informed by a large and growing literature focused on the complexities involved in modelling a wide range of species responses to climate change. Further, because the assumptions and limitations involved are likely to be similar, at least in kind if not to the same degree, application of niche modelling to a species as widespread and well known as humans may also provide insight into the implicit logic and general limitations of niche modelling in ecology.

Humans are globally distributed, but human population density is regionally variable. Accordingly, the distribution of human population density provides a more appropriate basis for niche modelling than the range distribution of human presence. However, because humans live in such a wide range of climatic conditions and are socio-economically diverse, the relationship between climate and human density is likely to differ in different parts of the world (Diamond, 2004; Fagan, 2004). For example, human population densities might be higher in cool localities in warm parts of the world or wet localities in dry parts of the world. Furthermore, the strength of association between climate and human populations is unlikely to be globally uniform, with human density more closely correlated with climate in some parts of the world than others. Finally, similar to the scale dependence of many ecological patterns (Schneider, 2001; McGill, 2010), the nature of correlations between climate and human populations is likely to vary according to the scale of comparison. In particular, the local distribution of human population density (e.g. over scales of tens to hundreds of kilometres) is likely to be dictated by non-climatic and historical factors such as proximity to waterways, trade routes and geological features, whereas across larger scales of comparisons (e.g. hundreds to thousands of kilometres) these factors are more likely to generate localized exceptions within a broader pattern of density distribution, which may be correlated with larger-scale environmental gradients such as climate. These forms of spatial non-stationarity (Fotheringham *et al.*, 1996) in the relationship between human populations and climate require a spatially explicit modelling approach, such as geographically weighted regression (Fotheringham *et al.*, 2002), in which regression parameters have enough spatial flexibility to reflect regional differences in human–climate associations. The alternative of standard regression models is inherently imprecise because regional differences are treated as noise rather than informative spatial patterns.

Here we assess the potential impacts of climate change on human populations by combining current regional relationships between climate and human population density with predicted regional climate change (Fig. 1). The key assumptions to this approach are that: (1) favourable climate conditions are currently associated with high population density and unfavourable climate conditions are associated with low population density, and (2) the impacts of climate change on human populations will be more severe where climate conditions currently associated with high population density decline rather than expand. These assumptions are not inconsistent with the existence of many additional non-climatic determinants of human population density, such as land use and agricultural production, distance from trading routes and natural resources (Small & Cohen, 2004; Nelson *et al.*, 2006; Ramankutty *et al.*, 2008; Beck & Sieber, 2010), nor of many additional non-climatic determinants of human vulnerability to climate change, such as

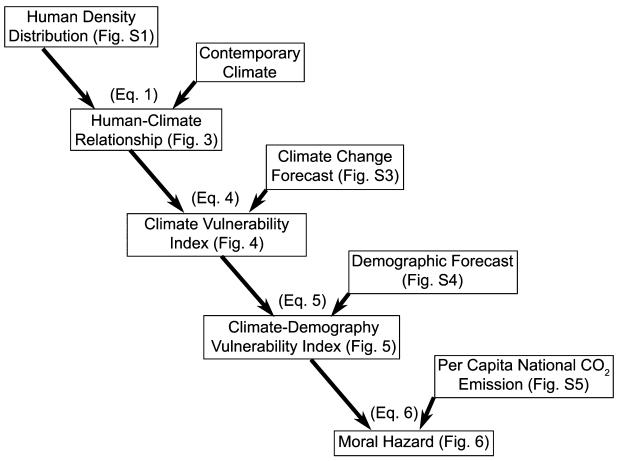

Figure 1 Conceptual framework of a spatially explicit approach for predicting the impacts of climate change on human populations. Rectangles represent data or indices calculated by the equations above each rectangle (see Methods). The climate vulnerability index (CVI) is estimated by combining climate change forecasts with current relationships between human density and climate. We further refined the CVI by contrasting predicted vulnerabilities with demographic growth rates to create a climate–demography vulnerability index (CDVI) reflecting the spatial disparities between demographic trends and climate-consistent population growth. This CDVI is then compared with per capita CO_2 emissions on a nation-by-nation basis to test the hypothesis of a moral hazard in climate change mitigation policies.

regional differences in exposure, sensitivity and resilience to climate change (Turner *et al.*, 2003). But we do assume that the many and complex socio-economic determinants of the distribution of human populations and their vulnerability to climate change are best considered not only in relation to how much climate is expected to change but also in the context of the match or mismatch between regional climate suitability and regional climate change.

First, we empirically examine how much of the global variation in human population density can be explained by climate variables, which climate variables offer the most explanatory power, and the nature and extent of regional variation in relationships between climate and population density. Second, we examine the importance of agricultural production as a potential covariate in relationships between climate and human population density. Third, we develop a climate vulnerability index (CVI) by combining regional climate–density relationships with predicted regional climate change. High vulnerability is predicted for regions where climate change will cause a decline in conditions currently associated with high population density and an increase in conditions associated with low population density. Fourth, since regions with rapid population growth are likely to be most severely affected by climate change (Raleigh & Urdal, 2007), we build on the CVI to develop a climate–demography vulnerability index (CDVI) that also incorporates current demographic trends. In this case, high vulnerability is predicted for regions where a decline in climate conditions currently supporting high population density is combined with rapid population growth. Finally, we relate this CDVI to current per capita greenhouse gas emissions as an initial quantification of potential moral hazards involved in climate change mitigation policies. If moral hazard represents a reduced incentive for actors to minimize risk if they are unlikely to bear the most negative potential outcomes of their actions (cf. Dembe & Boden, 2000), then a negative correlation between the causes and potential consequences of climate change is consistent with a moral hazard (or at least a perverse incentive structure; Rauchhaus, 2009) in climate change mitigation.

METHODS

Data source

Human densities in 1990 and 2015 were obtained through the third revision of the Gridded Population of the World (GPW) dataset adjusted to United Nations national population size (CIESIN, 2005). The extrapolation methods in the GPW dataset are based on population data obtained in the most recent subnational censuses from nearly 400,000 administrative units with average input resolution of 18 km and adjusted to national population sizes forecast in 2015 by the United Nations. We used a 1° resolution grid describing 18,504 georeferenced human densities (Fig. S1 in Supporting Information).

Climate data for current conditions (1950–2000 average) and general circulation model forecasts for 2050 were obtained from WorldClim, version 1.4 (Hijmans *et al.*, 2005). We used the 10 arcmin resolution consisting of 587,000 data points and filtered the dataset through our georeferenced human dataset to obtain 15,842 pairs of climate and human data. The reduced sample size produced by combining both datasets is due to the spatial mismatch in available data for islands and coastal areas.

Geographically weighted regression models

We used geographically weighted regression (GWR) to describe the spatial non-stationary nature of the current human–climate relationship. Our statistical models correlate 1990 human densities with a few climate variables that are geographically weighted to allow spatial flexibility in their respective regression coefficients. Take, for example, a model with four predictors: annual mean temperature (°C) (Tavg), mean temperature diurnal range (°C) (Trange), total annual precipitation (mm) (Ptot) and precipitation seasonality (Psea). Current human–climate relationships are then predicted by the following spatially explicit regression model:

$$\begin{aligned}\mathrm{density}_{\mathrm{lat,long}} = {} & \beta_{0(\mathrm{lat,long})} + \beta_{\mathrm{Tavg(lat,long)}}\mathrm{Tavg}_{\mathrm{lat,long}} \\ & + \beta_{\mathrm{Trange(lat,long)}}\mathrm{Trange}_{\mathrm{lat,long}} + \beta_{\mathrm{Ptot(lat,long)}}\mathrm{Ptot}_{\mathrm{lat,long}} \\ & + \beta_{\mathrm{Psea(lat,long)}}\mathrm{Psea}_{\mathrm{lat,long}} + \varepsilon_{\mathrm{lat,long}}.\end{aligned} \quad (1)$$

Local regression coefficients are estimated as:

$$\hat{\beta}_{(\text{lat,long})} = (X^{\mathrm{T}} W_{(\text{lat,long})} X)^{-1} X^{\mathrm{T}} W_{(\text{lat,long})} \text{density}_{(\text{lat,long})} \quad (2)$$

where X represents the matrix of predictors and W represents the matrix of geographical weights for each of the observed data used at a given location. We used a bi-square geographical weighting function as shown in equation 3:

$$\begin{aligned} w_{\text{lat,long}} &= [1-(d_{\text{lat,long}}/b)^2]^2 \quad \text{if} \quad d_{\text{lat,long}} < b \\ &= 0 \quad \text{otherwise} \end{aligned} \quad (3)$$

where w represents the weight of observed datum, d is the distance between the observed datum and the area where local regression parameters are estimated and b is a threshold distance referred to as the bandwidth.

We assessed the predictive power of 19 climate variables at various bandwidths with the software SAM (Rangel *et al.*, 2006). The bandwidth is limited to a minimum value by high spatial collinearity in predictor values while very large bandwidths cannot describe non-stationary patterns. A bandwidth of 27° (*c.* 3000 km) was chosen to maximize overall fit of regression models and minimize idiosyncratic regional patterns (Fig. S2, Tables S1 & S2). We had to divide the global dataset in four regions (at 44° and 94° longitude and isolating the Americas; mapped on Fig. 3) because of computing limitations arising with large matrices (see equation 2). We adjusted the geographic coverage of the four datasets by overlapping data by 17° to minimize the edge effect in estimates of the regression coefficient around division lines. We selected two models with both high regional significance (defined in Table S2) and predictive power but with contrasting climate variables to ensure that our results are robust to the selection of climate variables.

Indirect influence of agriculture

We evaluated the importance of agriculture as an indirect predictor of human density by modelling human density with both climate and agricultural variables. Based on the Ramankutty *et al.* (2008) gridded agricultural dataset, we created an agricultural density index by combining the proportion of land used for crops and pastures in 2000. We contrasted the explanatory power and the standardized regression coefficients of climate variables obtained with a climate model and a climate–agriculture model.

Climate vulnerability index

We forecast human densities in 2050 with equation 1 using the regression coefficients from current human–climate models and climate forecast data for 2050 (Fig. S3). From this climate-consistent forecast, we estimated annual growth rates of regional human density between 1990 and 2050 as follows:

$$\lambda_c = e^{[\ln(hd_{2050})/\ln(hd_{1990})]/60} \quad (4)$$

where λ_c represents the annual growth rate of climate-consistent human density (referred to herein as the CVI) and *hd* represents predicted human density based on equation 1.

Climate–demography vulnerability index

We created a CDVI reflecting the concordance between annual growth rates of climate-consistent human density (λ_c from equation 4) and annual growth rates of human density between 1990 and 2015 based on demographic models (λ_d) (Fig. S4). We calculated λ_d with equation 4, taking into account the different temporal horizon and had to limit its geographical coverage to regions of non-zero human density in the 1990 human density dataset. The CDVI is thus:

$$\text{CDVI} = \lambda_d - \lambda_c. \quad (5)$$

Regional CDVI values are consequently positive where annual growth rates of climate-consistent human density are lower than annual growth rates of human density predicted by demographic models.

Moral hazard

We used a linear regression model to evaluate the relationship between the cause and the predicted consequence of climate change. Given the lack of a gridded greenhouse gas emission dataset, we defined the cause of climate change based on national per capita CO_2 emissions in 2006 from the International Energy Association (IEA) estimates under the sectorial approach (OECD/IEA, 2008). We transformed the IEA data to national per capita CO_2 emissions using national population size and national boundaries in 2006 from United Nations Population Division (UNPD) (Fig. S5) (UNPD, 2007). Excluded from this analysis are 72 nations, collectively representing less than 2.7% of the world's population in 2006, with UN membership but without CO_2 emission data. We averaged gridded national CDVI values to test the moral hazard hypothesis with the following regression model where NPCE represents national per capita CO_2 emission:

$$\text{CDVI} = \beta_0 + \beta_{\text{NPCE}} \text{NPCE}. \quad (6)$$

Climate forecast uncertainties

To assess the robustness of CVI and CDVI to regional climate change uncertainties, we used two other sources of climate forecasts (CSIRO, HADCM3) in addition to the CCCMA 2a2 forecast presented in the main text. In all cases, we used WorldClim climate data based on the A2 emissions scenario and the 2050 horizon (Hijmans *et al.*, 2005).

RESULTS

Evaluation of the relationship between gridded global human density and climate using geographically weighted regression

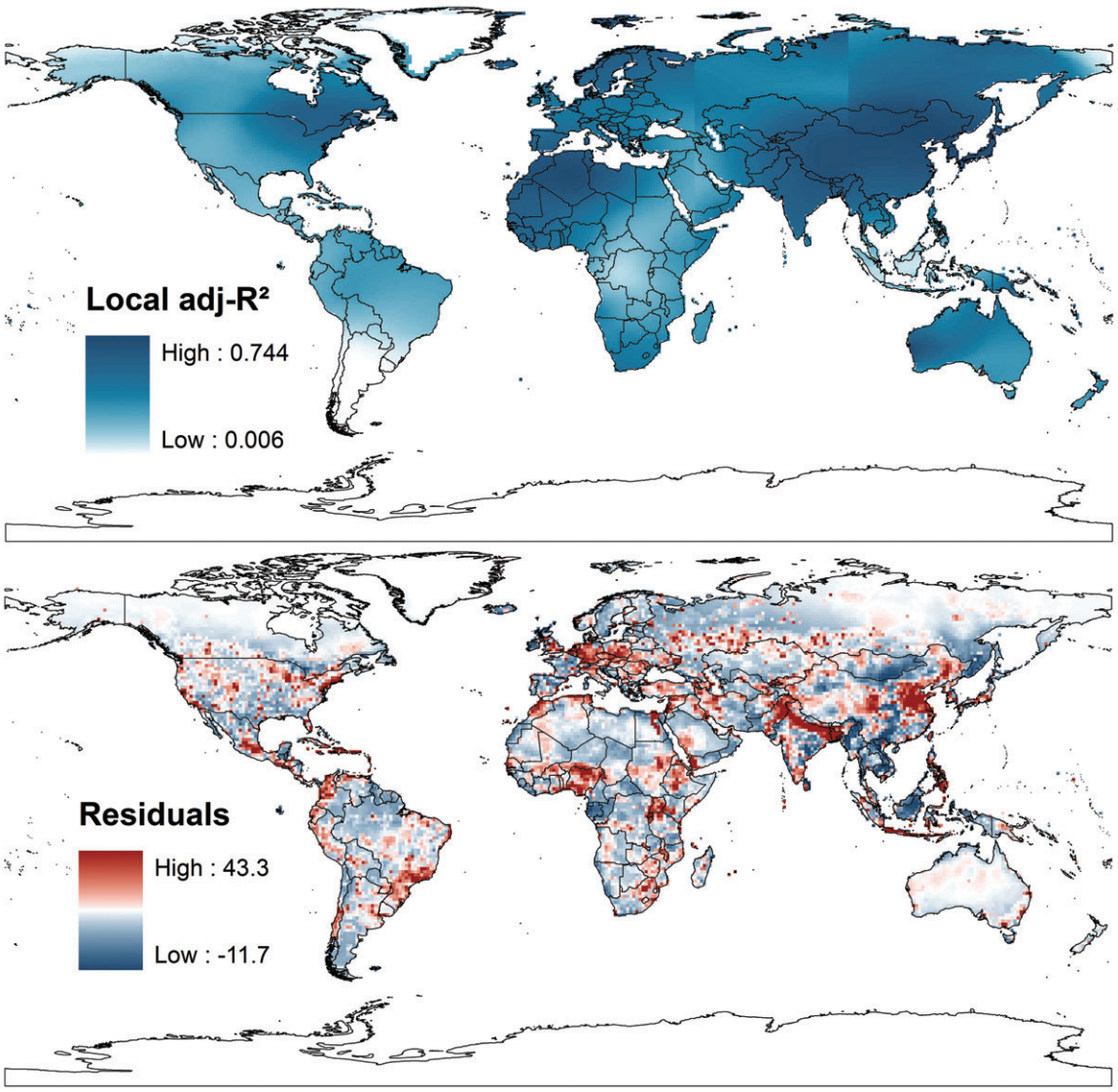

Figure 2 Global variation in explanatory power (local adjusted R^2) and residual values (observed density – predicted density) of a GWR model representing 1990 human densities based on four climate predictors (Fig. 3). The average (standard deviation) of local adj-R^2 and residual values are, respectively, 0.35 (0.17) and 0.11 (3.23).

reveals that approximately half of the global variation in human density can be accounted for by four climate variables (Table S2). Regions of high and low explanatory power were widely dispersed across the globe and not obviously related to population density or climate conditions (Fig. 2). The spatial pattern of climate–density residuals (actual density – climate-predicted density) does not reveal large-scale deviations in population density that are not accounted for by climate, but does indicate many localized areas where population density is much higher or lower than predicted from climate alone (Fig. 2). The spatial patterns of standardized regression coefficients relating climate predictors to population density are non-stationary (P-values < 0.001 across all models) with major continental isoclines of shifting coefficient signs (Fig. 3). In general, human population density tends to be negatively related to average annual temperature in warm parts of the world (e.g. northern South America and Africa in Fig. 3a) but positively related in cold parts of the world (e.g. high latitudes in Fig. 3a). Similarly, human population density tends to be negatively related to total annual precipitation in wet parts of the world (e.g. north-eastern North America and Southeast Asia in Fig. 3c) but positively related in dry parts of the world (e.g. central North America and the Middle East in Fig. 3c). This is not surprising, but the spatial change in relationships is not captured by most regression techniques given their stationary nature (Small & Cohen, 2004; Beck & Sieber, 2010).

Agricultural influence

The explanatory power of our climate model of current human density (adj-R^2 = 58%) was similar to the one (adj-R^2 = 61%) obtained by adding agricultural density (i.e. a combination of

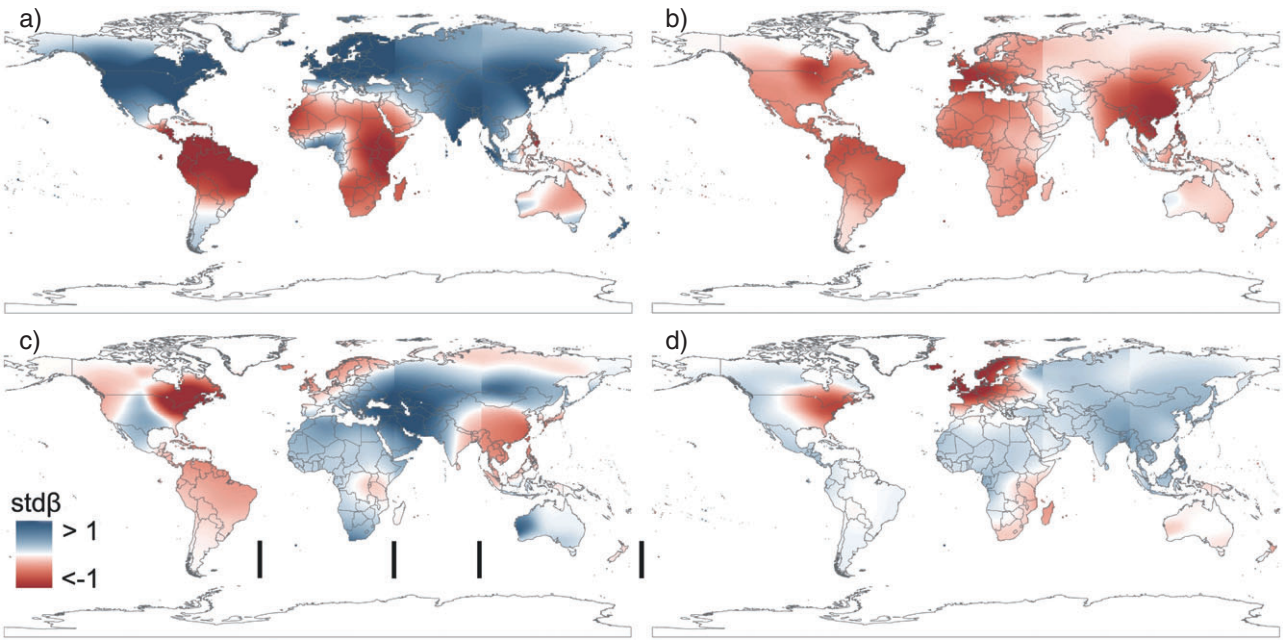

Figure 3 Geographically weighted regression analysis of the current relationship between human population density and four climate variables (adj-R^2 = 58%). Panels illustrate standardized regression coefficients (stdβ) for (a) annual mean temperature (°C), (b) mean temperature diurnal range (°C), (c) total annual precipitation (mm), and (d) precipitation seasonality (coefficient of variation). The average and range of stdβ for each variable are: (a) 0.29, −1.9 to 7.7; (b) −0.31, −2.5 to 0.3; (c) 0.07, −1.7 to 1.3; (d) 0.04, −1.8 to 5.6. The black lines at the bottom of panel (c) represent the longitudinal breaks in the global dataset and apply to all four panels (see Methods).

both crop and pasture density) as an additional predictor. Using crop density and pasture density as two separate and additional predictors incrementally improved the explanatory power (adj-R^2 = 67%). However, the four climate variables included in our model also explained considerable variation in crop density (adj-R^2 = 61%) and pasture density (adj-R^2 = 57%), suggesting that human density is influenced by climate conditions and agricultural density in a highly collinear pattern. The standardized regression coefficients of the four climate variables from the climate-only and the climate–agriculture models were highly correlated [average Pearson's correlation coefficient of 0.93 (range 0.87–0.97) with an average slope of 0.82 (range 0.77–0.89)]. Thus, although including agricultural density in our climate model decreases the explanatory power of climate predictors by about 20%, the regional patterns of climate variable regression coefficients remains unchanged (Figs 3, S6 & S7).

Climate vulnerability index

Regions with high CVI (i.e. where climate conditions currently associated with high population densities will shift towards climate conditions associated with low population densities) include central South America, the Middle East and both eastern and southern Africa (Fig. 4). Regions with low CVI are, on the other hand, largely restricted to northern portions of the Northern Hemisphere. Localized anomalies in predicted CVI near areas classified as having zero population density, such as central Brazil and central China, are artefacts caused by the increased sensitivity of growth rates estimated for very small predicted human densities.

Climate–demography vulnerability index

The CDVI magnifies the high CVI in regions where demographic forecasts of population growth are high, such as central South America, the Arabian Peninsula, Southeast Asia and much of Africa (Fig. 5). Regions with low CVI, including north-central North America, northern Europe and central Asia, also tend to have the most favourable CDVI because most of these regions are experiencing stable or even declining demographic growth rates.

Model robustness

We evaluated the robustness of our analyses with respect to the selection of predictors by comparing two models with contrasting sets of climate variables. The spatial patterns of standardized regression coefficients strongly differed between models (Figs 3 & S8), but the spatial patterns of CVI and CDVI of both models were very similar (Figs 4, 5, S9 & S10). The CVI and CDVI were also robust to current uncertainties in forecast climate change (Figs S11 & S12).

Moral hazard

We found a significant negative correlation between national per capita CO_2 emissions and national average CDVI, supporting

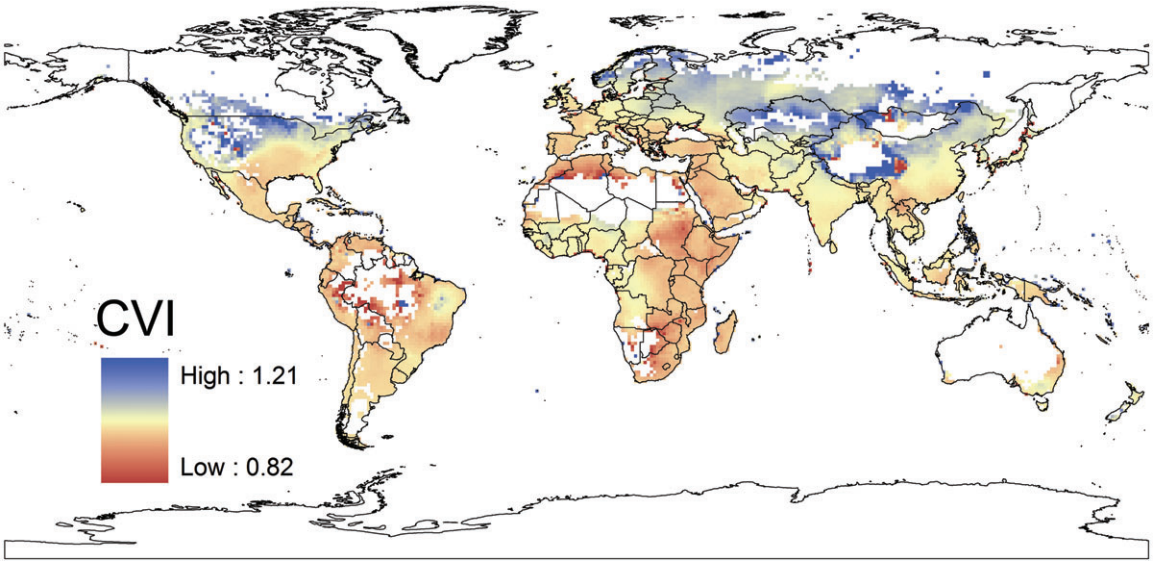

Figure 4 Climate vulnerabilities index (CVI) expressed as climate-consistent annual growth rate (λ_c; see equation 4) based on current human density–climate relationships (Fig. 3) and a 2050 climate forecast (Fig. S3a). Climate-consistent annual growth rates of less than one, indicated in red, represent negative growth and high vulnerabilities, while changes in annual growth rates of greater than one, indicated in blue, represent positive growth and low vulnerabilities. White regions correspond to human density values of zero in the global gridded population database.

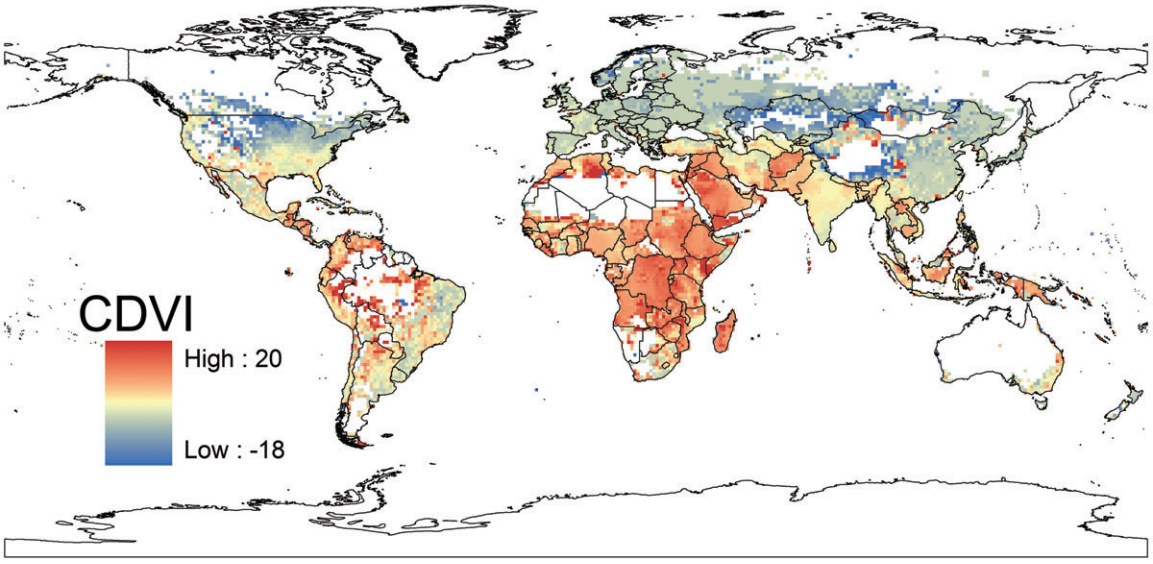

Figure 5 Global climate–demography vulnerability index (CDVI) estimated by subtracting CVI (Fig. 4) from demographic annual growth rates (Fig. S4), expressed as annual growth rates of human population density (see equation 5). Highly negative values, indicated in blue, represent low-vulnerability situations where current demographic growth is much lower than climate-consistent population growth, while highly positive values, indicated in red, represent high-vulnerability situations where current demographic growth vastly exceeds climate-consistent population growth. White regions correspond to human density values of zero in the global gridded population database.

the moral hazard hypothesis that countries predicted to be most negatively impacted by climate change are contributing the least to greenhouse gas emissions (Fig. 6). The explanatory power of this relationship is relatively low ($R^2 = 28\%$) indicating substantial variation in predicted impacts of climate change, at a national level, for a given per capita CO_2 emission.

DISCUSSION

The human impacts of climate change are likely to be most severe in parts of the world where current demographic growth is rapid and future climate change will amplify and expand conditions currently supporting low human population densi-

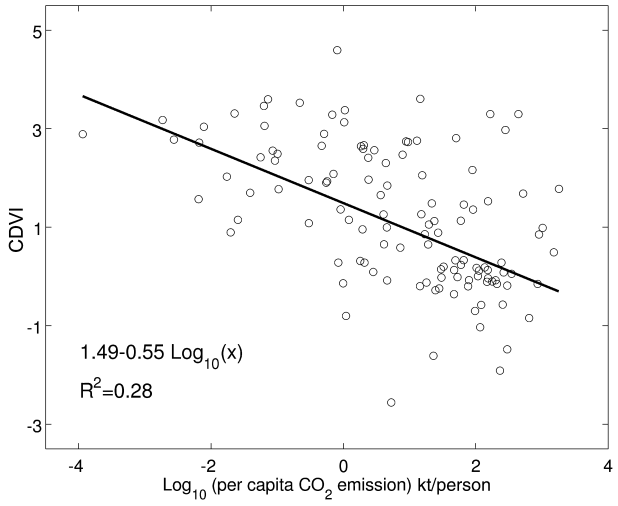

Figure 6 Relationship between per capita CO_2 emissions (kt per person) and average climate–demography vulnerability index (CDVI) among 120 nations ($P < 0.001$). The per capita CO_2 emissions are based on OECD/IEA 2006 national CO_2 emissions (OECD/IEA, 2008) and UNPD 2006 population size (UNPD, 2007) (Figure S5). Excluded from this analysis are 72 nations, collectively representing less than 2.7% of the world's population in 2006, with UN membership but without CO_2 emissions data.

ties. Our global analysis identifies hot and arid regions that will become hotter and drier in the future as being particularly vulnerable. This prediction is far from surprising. Nevertheless, the observation that regions of greatest vulnerability are generally distant from the high-latitude regions where the magnitude of climate change will be greatest and generally distinct from the nations responsible for most greenhouse gas emissions has important implications for climate adaptation and mitigation policies. On the other hand, our analysis indicates that many cold parts of the world with low population density have the potential to support higher population densities in a climate-changed future.

Similar to most current research on the ecological impacts of climate change using niche models (Austin *et al.*, 1984; Guisan & Thuiller, 2005; Austin *et al.*, 2006), the reliability of our analyses is a function of both data quality and underlying assumptions. The quality of current data on human population density (CIESIN, 2005) and global climate data (Hijmans *et al.*, 2005) is likely to be very high at the spatial resolution used in this study. Further, our demonstration that predicted patterns of climate vulnerability are highly congruent across two sets of climate predictors and three general circulation models indicates that these predictions are robust to current uncertainties in forecast climate change and climatic correlates of human population density (Fig. S11). However, the adequacy of our underlying assumptions requires careful evaluation. The main criticisms of ecological niche models are that they assume species to be at quasi-equilibrium with current climate, that they sometimes interpret species–climate correlations as causal, and that they assume instantaneous responses to climate change (Pearson & Dawson, 2003; Hampe, 2004). We now consider each of these assumptions in turn.

Current human–climate relationships

The complexities of human societies and the rapidity of their demographic and technological transitions make it unlikely that the distribution of human population density is at quasi-equilibrium with current climate. However, a small number of climate variables account for a surprisingly high proportion of global variation in current human density. The proportion of variance in current human density explained by our climate models varied between 40% and 60%, with an average of 54% (Table S2). Such explanatory power is favourably comparable with climate modelling of other species. For example, Iverson *et al.* (2008) modelled the current abundance of 134 tree species in the eastern United States based on 38 climatic and non-climatic variables and the pseudo-R^2 of their random forest models averaged 29% (standard deviation = 21%). The same research group also modelled 150 bird species in the same region based on climatic, elevation and tree abundance variables and their mean model had a pseudo-R^2 of 66% (standard deviation 15%; Rodenhouse *et al.*, 2008). If such predictive powers are considered to provide a satisfactory empirical basis to generate coarse initial predictions of bird and tree distributions in a climate changed future, then, a fortiori, our models suggest the same techniques can be usefully applied to humans (despite all of the events of recent centuries that could have served to decouple contemporary human density from contemporary climates). The capacity of climate conditions to predict the geographical distribution of human density has also been indirectly supported based on the relationships between climate, land use and human density across the Old World and Australia (Beck & Sieber, 2010). The reason why our simple climate–density models performed well, despite the absence of historical, economic or cultural components, probably relates to the importance of spatial scale and spatial flexibility in explaining biogeographical patterns (Schneider, 2001; McGill, 2010).

We analysed the relationship between climate and human density over large spatial scales, which reduces the importance of more localized determinants of population density such as proximity to waterways, trade routes, geological features and areas of industrial and agricultural development. The spatial scale of our models cannot describe highly localized and drastic variations in human density (e.g. the Nile and Ganges valleys, large cities); as a result urban areas and other localized forms of population aggregation are largely contributing to unexplained variation in our models. These factors are clearly important determinants of smaller-scale patterns in human density distribution and are likely to account for why significant amounts of variation remain unexplained by our models. The residuals of our climate–density model (Fig. 2) clearly illustrate localized regions where population density is higher or lower than expected based on climate variables. This map may be of interest to researchers interested in moving beyond simple climate-

based explanations of human density distribution to explore the multitude of historical, cultural, economic and geographic determinants of density distribution. Vulnerability to climate change will also be heavily influenced by fine-scale patterns in the distribution of human population density, including urbanization (McGranahan *et al.*, 2007; Satterthwaite, 2009), distance from coastlines related to sea-level rise (Nicholls & Lowe, 2004) and access to freshwater (World Water Assessment Programme, 2009). But these issues are probably best investigated with targeted regional models rather than by attempting to modify global models to include all factors of potential regional importance. In any event, our global representations of climate vulnerability are based, and should be interpreted, at a broad regional scale similar to the scale at which climate conditions vary.

Second, we used a spatially explicit modelling approach capable of analysing spatial non-stationarities in human–climate relationships rather than treating these as noise in a global model. The capacity for geographically weighted regression to capture the geographical variability in the magnitude and direction of human–climate relationships significantly decreased the spatial autocorrelation of residual values while providing visual insights into the spatial pattern of the influence of climate conditions. The non-stationary nature of this regression technique is also important in modelling species with a broad distribution, such as humans, because it does not rely on the assumption that there is no local adaptation. This often unrealistic assumption may also explain why stationary models of species with a broad distribution are generally weaker than those of species with a limited distribution (Newbold *et al.*, 2009).

Causality in species–climate correlations

One of the most fundamental criticisms of ecological niche modelling is that current species–climate relationships may not persist in a changing climate because they are not direct, causal relationships. Although future projections are difficult to test, empirical support for climate-based modelling of a variety of plant and animal taxa has been shown by predicting the non-native ranges of invasive species based on the climatic niche of their native range (Peterson, 2003; Thuiller *et al.*, 2005; but see Broennimann *et al.*, 2007; Fitzpatrick *et al.*, 2007). Palaeoclimate studies also reveal a surprising degree of coherence between species assemblages and prevailing climate conditions, even during periods of relatively rapid climate change (though unlikely to be as rapid as the anthropogenic warming occurring during this and the previous century) (McGlone, 1996; Araújo *et al.*, 2008). Finally, recent climate change has been shown to coherently drive a wide range of ecological phenomena, despite the importance of many non-climate determinants (Parmesan & Yohe, 2003).

The validity of our climate vulnerability indices requires sufficient continuity in the influences of climate on human populations that the climate vulnerability of human populations in a climate-changed future will be related, in some way, to the current climatic correlates of human density. The high explanatory power of our models of current human populations may be driven by non-climate variables that are influenced by climate. If this were the case, our indices would only be meaningful if the climate relationships of these non-climate variables remained consistent in a changing climate. Localized socioeconomic variables such as concentrated areas of resource exploitation, transportation, trade or economic development are likely to contribute to unexplained variation in our models, rather than as globally coherent covariates of the density–climate relationship, given the relatively smooth changes in the regression coefficients of climate predictors (Figs 3, S6 & S8). Agricultural and large-scale socio-economic variables are better candidates for globally important covariates of the climate–density relationship, because they have global relevance and are more likely to vary across large spatial scales in a pattern similar to climate variables.

Food production has been central to the foundation and persistence of human societies (Diamond, 2004), and its strong association with climate conditions has lead to climate change models predicting substantial regional changes in food production (Thomas, 2006; Cline, 2007). Additionally, cropland and pastures now represent approximately 40% of the land surface (Foley *et al.*, 2005) and may therefore strongly influence the geographical distribution of human density. Our climate-based models of current agricultural density support the hypothesis of strong climate–agriculture relationships. On the other hand, our analysis indicates that the climatic correlates of human density are strongly overlapping with climatic correlates of agricultural output. Thus, at a global scale of analysis agricultural density explains little additional variation in human density that is not already explained by climate. This overlap in explanatory power, knowledge that not all the impacts of climate on human populations operate via agriculture, and the absence of gridded global agricultural forecasts have led us to focus on predictions of climate vulnerability derived from density–climate relationships for the time being. However, the past, current and presumably future distribution and well-being of human populations is likely to be as dependent on the availability of food resources as that of any other animal population. As a result, more thorough examination of the inter-relationships between climate, the production and distribution of food resources, and the density distribution and vulnerability of human populations clearly warrants deeper consideration. Climate conditions have recently been shown to better explain current land-use patterns than soil type in the Old World and Australia (Beck & Sieber, 2010). Although Beck & Sieber (2010) did not model current human density with climate variables, their models of human density based on land-use variables performed relatively well (adj-R^2 = 34%).

In many regions of the world, forms of socio-economic development and employment opportunities seemingly unrelated to either climate or agriculture may be primary current drivers of human density distribution. The emergence of these density drivers may only partially erode current correlations between climate and density if development and employment tends to

arise in localities with a long history of dense human occupation, which may have originally been predicated on climate or agricultural suitability. The emergence of major economic and employment opportunities in previously unoccupied, climatically unfavourable regions of the world would do much more to weaken current associations between climate and human population density. But to the extent that these remain localized concentrations of higher than expected density in vast regions of otherwise low density, they are unlikely to be important influences in global analyses of human density distribution.

A more important and uncertain issue is how socio-economic factors will interact with modern climatic correlates of population density and regional climate change to define the climate vulnerability of human populations. In this paper, we considered only one socio-economic factor, projected population growth rates derived from demographic forecasts, in our analyses. Inclusion of this socio-economic variable to create our CDVI index tended to reinforce and amplify the regional disparities predicted from our CVI index based on climate and density alone. That is, regions where climate conditions currently supporting high population density are expected to decline also tend to be characterized by higher than average population growth. Thus, comparison of CVI and CDVI maps reveals a similar global pattern but the magnitude of disparity tends to be higher after the inclusion of one socio-economic variable. But many more socio-economic variables can and should be considered. For example, recent research has examined the importance of climate conditions on national institutions (Sokoloff & Engerman, 2000; Acemoglu *et al.*, 2002), associations between trade policy and economic development (Frankel & Romer, 1999), and relationships between national institutions, environmental endowments and economic development (Easterly & Levine, 2003).

Instantaneous response

Climate change predictions based on ecological niche models are often criticized because they assume instantaneous responses of species to new climatic conditions (Pearson & Dawson, 2003). For example, if climate change leads to the appearance of suitable climatic conditions in a previously unoccupied location, species are assumed to be able to immediately occupy that locality. This assumption ignores potential limits to dispersal and the difficulty of establishing in sites that may lack key resources or habitats (because they may be lagged in their response or also be limited by non-climatic factors). Because our analysis focuses on human population density within already occupied areas, we circumvent the need for some of these assumptions. Nevertheless, our calculation of climate-consistent population growth involves a similar implicit logic that, as climate changes, so too will the potential for human population growth. However, in recognition of the many diverse drivers of human population growth and responses to climate change, we do not proceed to the step of using our climate modelling to predict the redistribution of human population density in a climate-changed future. Instead, we limit our analysis to the calculation of *potential* climate-consistent population growth as a basis to predict regions of relatively high and low vulnerability to climate change. Although our approach could be extended to predict migration patterns induced by climate change (Myers, 2002; McLeman & Smit, 2006), we caution about the need to differentiate potential from realized responses to climate change and the need to match the spatial scale of analyses to the spatial scale of interpretation.

CONCLUSIONS

The strength of current associations between human population density and climate conditions and the robustness of the climate vulnerability predictions they generate offer a critically needed framework for predicting regional disparities in the potential impacts of climate change on human populations. Assessments of regional vulnerability have been largely focused on the influence of GCM forecasts on adaptive capacities (IPCC, 2007; World Water Assessment Programme, 2009), but there is little doubt that treating exposure as simply the magnitude of change in one or a suite of climate variables is inadequate (Hockley *et al.*, 2009). Climate exposure should rather incorporate regional relationships between populations and climate, the direction and magnitude of regional climate change, as well as current and predicted demographic trends (McGranahan *et al.*, 2007; Meyerson *et al.*, 2007; Pope & Terrell, 2008). Additional insight into the human consequences of climate change can be achieved by expanding the framework described here to consider additional effects of climate change, such as sea level rise (Nicholls & Lowe, 2004; Overpeck *et al.*, 2006; Yin *et al.*, 2009) and extreme weather events (Hockley *et al.*, 2009; Sherwood & Huber, 2010) as well as measures of adaptive capacities in areas such as resource management systems or development initiatives (Smit & Wandel, 2006).

In summary, we believe that the capacity of our simple human ecological models to explain broad density distribution patterns provides a coarse but important way to formulate initial predictions of the impacts of climate change on human societies. These initial predictions can be used as a null model (Gotelli, 2001) to highlight the regional importance of historical, economic or social correlates of human density and vulnerability to climate change.

ACKNOWLEDGEMENTS

We are grateful to Elena Bennett for hardware support and Guillaume Larocque for analytical advice. We thank Henrique M. Pereira and two anonymous referees for their helpful comments. This research was supported by the Natural Sciences and Engineering Research Council of Canada (NSERC).

REFERENCES

Acemoglu, D., Johnson, S. & Robinson, J.A. (2002) Reversal of fortune: geography and institutions in the making of the modern world income distribution. *Quarterly Journal of Economics*, **117**, 1231–1294.

Adger, W.N. (2006) Vulnerability. *Global Environmental Change*, **16**, 268–281.

Araújo, M.B., Nogués-Bravo, D., Diniz-Filho, J.A.F., Haywood, A.M., Valdes, P.J. & Rahbek, C. (2008) Quaternary climate changes explain diversity among reptiles and amphibians. *Ecography*, **31**, 8–15.

Austin, M. (2007) Species distribution models and ecological theory: a critical assessment and some possible new approaches. *Ecological Modelling*, **200**, 1–19.

Austin, M.P., Cunningham, R.B. & Fleming, P.M. (1984) New approaches to direct gradient analysis using environmental scalars and statistical curve-fitting procedures. *Vegetatio*, **55**, 11–27.

Austin, M.P., Belbin, L., Meyers, J.A., Doherty, M.D. & Luoto, M. (2006) Evaluation of statistical models used for predicting plant species distributions: role of artificial data and theory. *Ecological Modelling*, **199**, 197–216.

Beck, J. & Sieber, A. (2010) Is the spatial distribution of mankind's most basic economic traits determined by climate and soil alone? *PLoS ONE*, **5**, e10416.

Broennimann, O., Treier, U.A., Muller-Scharer, H., Thuiller, W., Peterson, A.T. & Guisan, A. (2007) Evidence of climatic niche shift during biological invasion. *Ecology Letters*, **10**, 701–709.

Burke, M.B., Miguel, E., Satyanath, S., Dykema, J.A. & Lobell, D.B. (2009) Warming increases the risk of civil war in Africa. *Proceedings of the National Academy of Sciences USA*, **106**, 20670–20674.

Chase, T.N., Wolter, K., Pielke, R.A., Sr & Rasool, I. (2006) Was the 2003 European summer heat wave unusual in a global context? *Geophysical Research Letters*, **33**, L23709.

CIESIN (Center for International Earth Science Information Network , Columbia University, and Centro Internacional de Agricultura Tropical, CIAT) (2005) *Gridded population of the world version 3 (GPWv3): population density grids*. Socioeconomic Data and Applications Center (SEDAC), Columbia University, Palisades, NY. Available at: http://sedac.ciesin.columbia.edu/gpw (accessed 4 January 2009).

Cline, W.R. (2007) *Global warming and agriculture: impact estimates by country*. Peterson Institute, Washington, DC.

Costello, A., Abbas, M. & Allen, A. (2009) Managing the health effects of climate change. *The Lancet*, **373**, 1693–1733.

Dembe, A.E. & Boden, L.I. (2000) Moral hazard: a question of morality? *New Solutions*, **10**, 257–279.

Diamond, J. (2004) *Collapse: how societies choose to fail or succeed*. Viking, New York.

Dyson, T. (2005) On development, demography and climate change: the end of the world as we know it? *Population and Environment*, **27**, 117–149.

Easterly, W. & Levine, R. (2003) Tropics, germs, and crops: how endowments influence economic development. *Journal of Monetary Economics*, **50**, 3–39.

Fagan, B.M. (2004) *The long summer: how climate changed civilization*. Basic Books, New York.

Fitzpatrick, M.C., Weltzin, J.F., Sanders, N.J. & Dunn, R.R. (2007) The biogeography of prediction error: why does the introduced range of the fire ant over-predict its native range? *Global Ecology and Biogeography*, **16**, 24–33.

Foley, J.A., DeFries, R., Asner, G.P., Barford, C., Bonan, G., Carpenter, S.R., Chapin, F.S., Coe, M.T., Daily, G.C., Gibbs, H.K., Helkowski, J.H., Holloway, T., Howard, E.A., Kucharik, C.J., Monfreda, C., Patz, J.A., Prentice, I.C., Ramankutty, N. & Snyder, P. (2005) Global consequences of land use. *Science*, **309**, 570–574.

Ford, J.D. & Smit, B. (2004) A framework for assessing the vulnerability of communities in the Canadian arctic to risks associated with climate change. *Arctic*, **57**, 389–400.

Fotheringham, A.S., Charlton, M. & Brunsdon, C. (1996) The geography of parameter space: an investigation of spatial non-stationarity. *International Journal of Geographical Information Systems*, **10**, 605–627.

Fotheringham, A.S., Brundson, C. & Charlton, M. (2002) *Geographically weighted regression: the analysis of spatially varying relationships*. John Wiley and Sons, Hoboken, NJ.

Frankel, J.A. & Romer, D. (1999) Does trade cause growth? *American Economic Review*, **89**, 379–399.

Gotelli, N.J. (2001) Research frontiers in null model analysis. *Global Ecology and Biogeography*, **10**, 337–343.

Guisan, A. & Thuiller, W. (2005) Predicting species distribution: offering more than simple habitat models. *Ecology Letters*, **8**, 993–1009.

Hampe, A. (2004) Bioclimate envelope models: what they detect and what they hide. *Global Ecology and Biogeography*, **13**, 469–471.

Hijmans, R.J., Cameron, S.E., Parra, J.L., Jones, P.G. & Jarvis, A. (2005) Very high resolution interpolated climate surfaces for global land areas. *International Journal of Climatology*, **25**, 1965–1978.

Hockley, N., Gibbons, J.M., Edwards-Jones, G., Battisti, D.S. & Naylor, R.L. (2009) Risks of extreme heat and unpredictability. *Science*, **324**, 177–179.

Horridge, M., Madden, J. & Wittwer, G. (2005) The impact of the 2002–2003 drought on Australia. *Journal of Policy Modeling*, **27**, 285–308.

IPCC (2007) *Climate change 2007: the physical science basis. Contribution of Working Group I to the Fourth Assessment Report of the Intergovernmental Panel on Climate Change*. Cambridge University Press, Cambridge.

Iverson, L.R., Prasad, A.M., Matthews, S.N. & Peters, M. (2008) Estimating potential habitat for 134 eastern US tree species under six climate scenarios. *Forest Ecology and Management*, **254**, 390–406.

Kuper, R. & Kropelin, S. (2006) Climate-controlled Holocene occupation in the Sahara: motor of Africa's evolution. *Science*, **313**, 803–807.

Lobell, D.B., Burke, M.B., Tebaldi, C., Mastrandrea, M.D., Falcon, W.P. & Naylor, R.L. (2008) Prioritizing climate change adaptation needs for food security in 2030. *Science*, **319**, 607–610.

McGill, B.J. (2010) Matters of scale. *Science*, **328**, 575–576.

McGlone, M.S. (1996) When history matters: scale, time, climate and tree diversity. *Global Ecology and Biogeography Letters*, **5**, 309–314.

McGranahan, G., Balk, D. & Anderson, B. (2007) The rising tide: assessing the risks of climate change and human settlements in low elevation coastal zones. *Environment and Urbanization*, **19**, 17–37.

McLeman, R. & Smit, B. (2006) Migration as an adaptation to climate change. *Climatic Change*, **76**, 31–53.

Meyerson, F.A.B., Merino, L. & Durand, J. (2007) Migration and environment in the context of globalization. *Frontiers in Ecology and the Environment*, **5**, 182–190.

Myers, N. (2002) Environmental refugees: a growing phenomenon of the 21st century. *Philosophical Transactions of the Royal Society B: Biological Sciences*, **357**, 609–613.

Nelson, G.C., Bennett, E., Berhe, A.A., Cassman, K., DeFries, R., Dietz, T., Dobermann, A., Dobson, A., Janetos, A., Levy, M., Marco, D., Nakicenovic, N., O'Neill, B., Norgaard, R., Petschel-Held, G., Ojima, D., Pingali, P., Watson, R. & Zurek, M. (2006) Anthropogenic drivers of ecosystem change: an overview. *Ecology and Society*, **11**, 29.

Newbold, T., Reader, T., Zalat, S., El-Gabbas, A. & Gilbert, F. (2009) Effect of characteristics of butterfly species on the accuracy of distribution models in an arid environment. *Biodiversity and Conservation*, **18**, 3629–3641.

Nicholls, R.J. & Lowe, J.A. (2004) Benefits of mitigation of climate change for coastal areas. *Global Environmental Change: Human and Policy Dimensions*, **14**, 229–244.

OECD/IEA (2008) *CO_2 emissions from fuel combustion*. OECD, Paris, France.

Overpeck, J.T., Otto-Bliesner, B.L., Miller, G.H., Muhs, D.R., Alley, R.B. & Kiehl, J.T. (2006) Paleoclimatic evidence for future ice-sheet instability and rapid sea-level rise. *Science*, **311**, 1747–1750.

Parmesan, C. & Yohe, G. (2003) A globally coherent fingerprint of climate change impacts across natural systems. *Nature*, **421**, 37–42.

Patz, J.A., Campbell-Lendrum, D., Holloway, T. & Foley, J.A. (2005) Impact of regional climate change on human health. *Nature*, **438**, 310–317.

Pearson, R.G. & Dawson, T.P. (2003) Predicting the impacts of climate change on the distribution of species: are bioclimate envelope models useful? *Global Ecology and Biogeography*, **12**, 361–371.

Peterson, A.T. (2003) Predicting the geography of species' invasions via ecological niche modeling. *Quarterly Review of Biology*, **78**, 419–433.

Pope, K.O. & Terrell, J.E. (2008) Environmental setting of human migrations in the circum-Pacific region. *Journal of Biogeography*, **35**, 1–21.

Poumadère, M., Mays, C., Le Mer, S. & Blong, R. (2005) The 2003 heat wave in France: dangerous climate change here and now. *Risk Analysis: an International Journal*, **25**, 1483–1494.

Raleigh, C. & Urdal, H. (2007) Climate change, environmental degradation and armed conflict. *Political Geography*, **26**, 674–694.

Ramankutty, N., Evan, A.T., Monfreda, C. & Foley, J.A. (2008) Farming the planet: 1. Geographic distribution of global agricultural lands in the year 2000. *Global Biogeochemical Cycles*, **22**, GB1003.

Rangel, T.F.L.V.B., Diniz-Filho, J.A.F. & Bini, L.M. (2006) Towards an integrated computational tool for spatial analysis in macroecology and biogeography. *Global Ecology and Biogeography*, **15**, 321–327.

Rauchhaus, R.W. (2009) Principal-agent problems in humanitarian intervention: moral hazards, adverse selection, and the commitment dilemma. *International Studies Quarterly*, **53**, 871–884.

Rodenhouse, N., Matthews, S., McFarland, K., Lambert, J., Iverson, L., Prasad, A., Sillett, T. & Holmes, R. (2008) Potential effects of climate change on birds of the northeast. *Mitigation and Adaptation Strategies for Global Change*, **13**, 517–540.

Satterthwaite, D. (2009) The implications of population growth and urbanization for climate change. *Environment and Urbanization*, **21**, 545–567.

Schneider, D.C. (2001) The rise of the concept of scale in ecology. *Bioscience*, **51**, 545–553.

Service, R.F. (2009) Hydrology: California's water crisis: worse to come? *Science*, **323**, 1665.

Sherwood, S.C. & Huber, M. (2010) An adaptability limit to climate change due to heat stress. *Proceedings of the National Academy of Sciences USA*, **107**, 9552–9555.

Small, C. & Cohen, J.E. (2004) Continental physiography, climate, and the global distribution of human population. *Current Anthropology*, **45**, 269–277.

Smit, B. & Wandel, J. (2006) Adaptation, adaptive capacity and vulnerability. *Global Environmental Change*, **16**, 282–292.

Sokoloff, K.L. & Engerman, S.L. (2000) History lessons – institutions, factor endowments, and paths of development in the New World. *Journal of Economic Perspectives*, **14**, 217–232.

Thomas, A. (2006) Climatic change and potential agricultural productivity in China. *Erdkunde*, **60**, 157–172.

Thuiller, W., Richardson, D.M., Pyšek, P., Midgley, G.F., Hughes, G.O. & Rouget, M. (2005) Niche-based modelling as a tool for predicting the risk of alien plant invasions at a global scale. *Global Change Biology*, **11**, 2234–2250.

Trouet, V., Esper, J., Graham, N.E., Baker, A., Scourse, J.D. & Frank, D.C. (2009) Persistent positive North Atlantic oscillation mode dominated the medieval climate anomaly. *Science*, **324**, 78–80.

Turner, B.L., Kasperson, R.E., Matson, P.A., McCarthy, J.J., Corell, R.W., Christensen, L., Eckley, N., Kasperson, J.X., Luers, A., Martello, M.L., Polsky, C., Pulsipher, A. & Schiller, A. (2003) A framework for vulnerability analysis in sustainability science. *Proceedings of the National Academy of Sciences USA*, **100**, 8074–8079.

UNPD (United Nations Population Division) (2007) *United Nations Environment Programme/DEWA/GRID-Eurpoe*. UNEP, Geneva. http://www.grid.unep.ch

Weiss, H., Courty, M.-A., Wetterstrom, W., Guichard, F., Senior, L., Meadow, R. & Curnow, A. (1993) The genesis and collapse

of third millennium north Mesopotamian civilization. *Science*, **261**, 995–1004.

WHO (World Health Organization] (2004) *Using climate to predict disease outbreaks: a review*. WHO, Geneva.

World Water Assessment Programme (2009) *The United Nations world water development report 3: water in a changing world*. UNESCO Publishing, Paris.

Yin, J., Schlesinger, M.E. & Stouffer, R.J. (2009) Model projections of rapid sea-level rise on the northeast coast of the United States. *Nature Geoscience*, **2**, 262–266.

Zhang, D.D., Brecke, P., Lee, H.F., He, Y.-Q. & Zhang, J. (2007) Global climate change, war, and population decline in recent human history. *Proceedings of the National Academy of Sciences USA*, **104**, 19214–19219.

SUPPORTING INFORMATION

Additional Supporting Information may be found in the online version of this article:

Figure S1 Global distribution of human density.

Figure S2 Explanatory power and average regional significance of two current climate models of 1990 human densities as a function of geographically weighted regression (GWR) bandwidth.

Figure S3 Forecast changes in climate factors.

Figure S4 Annual growth rate of human population density between 1990 and 2015.

Figure S5 National average per capita CO_2 emissions.

Figure S6 Standardized regression coefficients (stdβ) for climate factors from a geographically weighted regression (GWR) model representing 1990 human densities based on four climate predictors (average 1950–2000) and agricultural extent *c.* 2000.

Figure S7 Standardized regression coefficients (stdβ) for agricultural extent from a geographically weighted regression (GWR) model representing 1990 human densities based on four climate predictors (average 1950–2000) and agricultural extent *c.* 2000.

Figure S8 Standardized regression coefficients (stdβ) for climate factors from a geographically weighted regression (GWR) model between 1990 human densities and four climate predictors (1950–2000 average).

Figure S9 Climate vulnerabilities index (CVI) expressed as climate consistent changes in annual growth rate of human population density based on a geographically weighted regression (GWR) model between 1990 human density and four climate predictors and a 2050 climate forecast.

Figure S10 Global climate–demography vulnerability index (CDVI) estimated by subtracting climate vulnerabilities from demographic annual growth rates, displayed as percentage of annual growth rates of human density.

Figure S11 Climate vulnerabilities (CVI) expressed as climate-consistent changes in annual growth rate based on two human–climate models and three general circulation models for 2050 under the A2 scenario.

Figure S12 Global patterns of climate–demography vulnerability index (CDVI) for two human–climate regression models and three general circulation models for 2050 under the A2 scenario.

Table S1 Climate variables used to predict contemporary human densities and the number of models including each variable.

Table S2 Explanatory power and regional significance of geographically weighted regression (GWR) models of current human densities based on current climate predictors.

As a service to our authors and readers, this journal provides supporting information supplied by the authors. Such materials are peer-reviewed and may be reorganized for online delivery, but are not copy-edited or typeset. Technical support issues arising from supporting information (other than missing files) should be addressed to the authors.

BIOSKETCH

Jason Samson is a PhD student at McGill University, Canada. His main research focus is on the ecological determinants of spatial patterns of abundance across species distributions. He is especially interested in developing novel methods to better understand the effects of climate change on the relationship between the environment and human societies through ecological models.

Editor: David Currie

Table S1. Climate variables used to predict contemporary human densities and the number of models including each variable. The variable code is used to name models in table S2.

Code	Climate predictor	# of models
1	Annual Mean Temperature (^{o}C)	20
2	Mean Temperature Diurnal Range (^{o}C)	5
3	Isothermality (%)	5
4	Temperature Seasonality (%)	6
5	Max Temperature of Warmest Month (^{o}C)	7
6	Min Temperature of Coldest Month (^{o}C)	7
7	Temperature Annual Range (^{o}C)	5
8	Mean Temperature of Wettest Quarter (^{o}C)	4
9	Mean Temperature of Driest Quarter (^{o}C)	4
10	Mean Temperature of Warmest Quarter (^{o}C)	4
11	Mean Temperature of Coldest Quarter (^{o}C)	4
12	Total Annual Precipitation (mm)	17
13	Precipitation of Wettest Month (mm)	6
14	Precipitation of Driest Month (mm)	7
15	Precipitation Seasonality (CV)	14
16	Precipitation of Wettest Quarter (mm)	4
17	Precipitation of Driest Quarter (mm)	4
18	Precipitation of Warmest Quarter (mm)	4
19	Precipitation of Coldest Quarter (mm)	4

Table S2. Explanatory power and regional significance of 33 GWR models of contemporary human densities based on current climate predictors. Adjusted coefficients of determination are calculated by averaging the adj-R^2 of the four datasets independently analysed (see Methods). The regional significance index is an average for the four datasets of the proportion of localities where the pseudo t-values (Fotheringham *et al.*, 2002*)* are larger than 2 for each climate predictor. Model descriptions are based on table S1. Selected models are in bold.

Model	Adj-R^2	Regional significance
hd=f(1,3,7,10,11)	0.582	53%
hd=f(1,2,4,5,6)	0.581	43%
hd=f(1,2,12,18,19)	0.579	52%
hd=f(1,2,12,15)	**0.575**	**65%**
hd=f(1,2,4,7)	0.568	51%
hd=f(1,5,6,12,15)	0.568	43%
hd=f(1,5,6,13,14)	0.568	42%
hd=f(1,5,6,16,17)	0.568	42%
hd=f(1,10,11,12,15)	0.567	48%
hd=f(4,7,10,11)	0.566	44%
hd=f(1,3,12,16,17)	0.565	48%
hd=f(1,4,12,16,17)	0.563	50%
hd=f(1,5,6,13)	**0.561**	**42%**
hd=f(1,7,12,15)	0.560	61%
hd=f(5,6,13,14)	0.560	48%
hd=f(1,8,9,12,15)	0.559	32%
hd=f(1,5,12,15)	0.559	56%
hd=f(1,3,13,14)	0.556	60%
hd=f(1,8,9,12,18,19)	0.555	30%
hd=f(10,11,12,15)	0.554	54%
hd=f(1,5,6,14)	0.553	42%
hd=f(1,3,18,19)	0.545	56%
hd=f(8,9,12,15)	0.542	59%
hd=f(1,5,6)	0.542	43%
hd=f(2,4,7,15)	0.529	51%
hd=f(1,12)	0.527	71%
hd=f(8,9,18,19)	0.522	60%
hd=f(12,13,14,15)	0.496	48%
hd=f(12,15,16,17)	0.495	49%
hd=f(13,14,15)	0.480	51%
hd=f(12,13,14)	0.480	51%
hd=f(12,15)	0.474	66%
hd=f(3,15)	0.422	61%

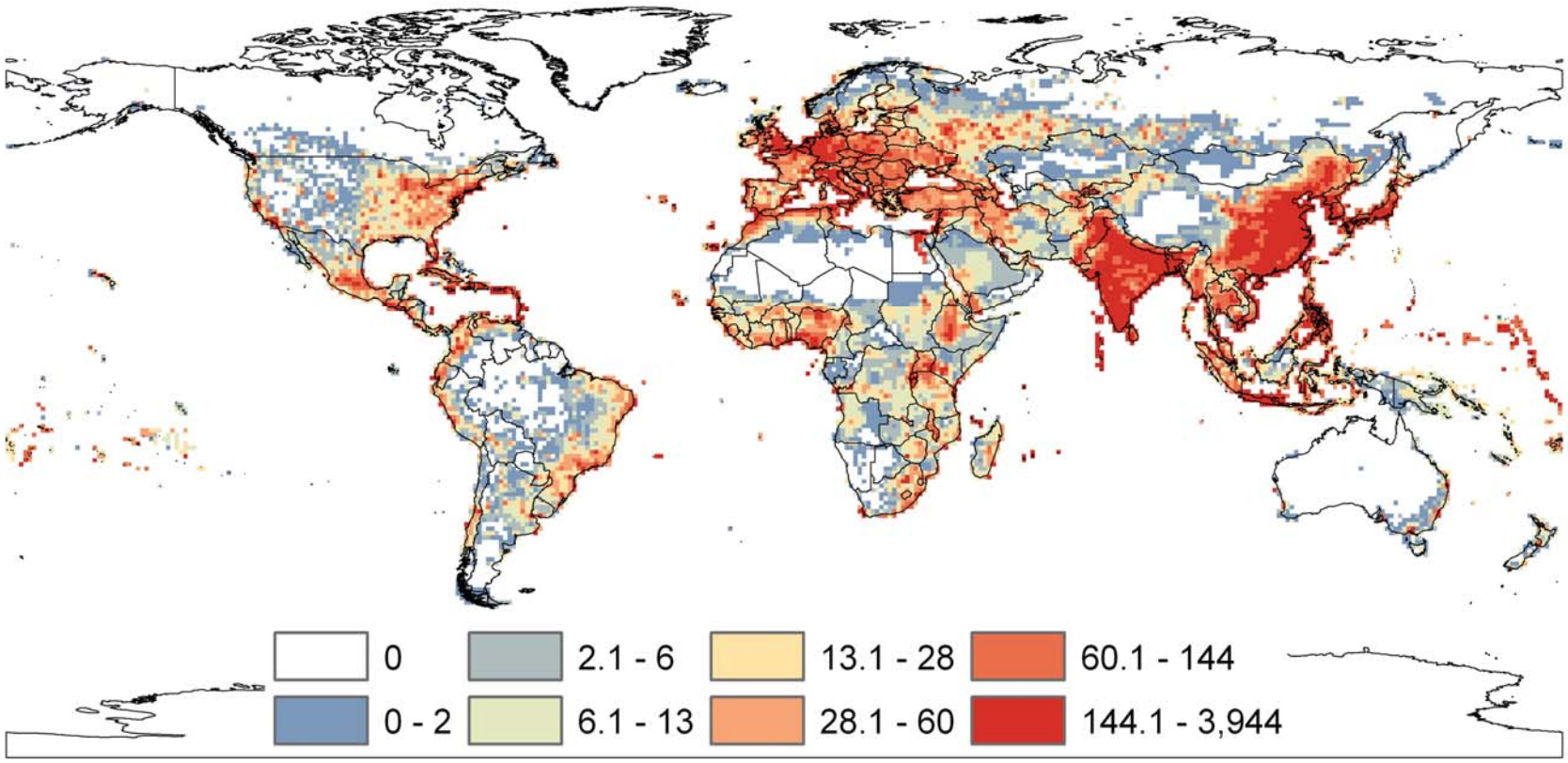

Figure S1. Global distribution of human density, expressed as persons per km^2, in 1990 at a resolution of 1^o (CIESIN, 2005).

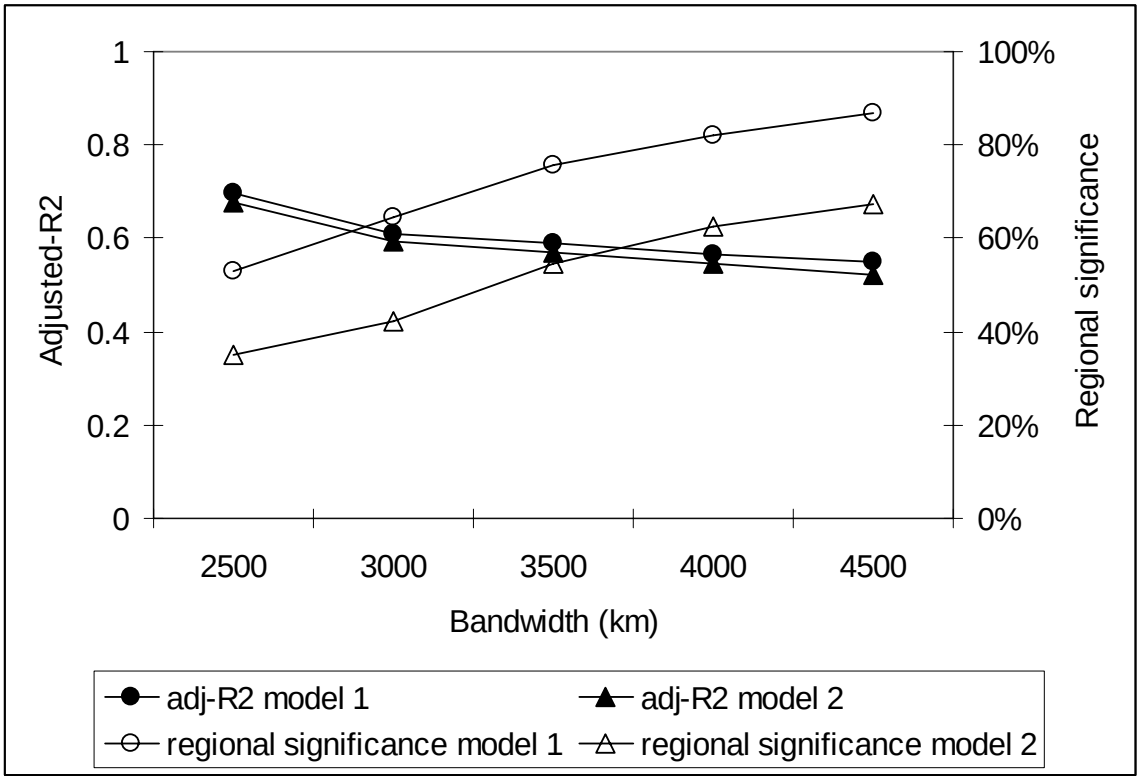

Figure S2. Explanatory power and average regional significance of two current climate models of 1990 human densities as a function of GWR bandwidth (model 1: *hd=f(1,2,12,15)*, model 2: *hd=f(1,5,6,13)*, see table S1 and S2) for the Old World, displayed as average of the three datasets analysed. The New World required a bandwidth based on an adaptive kernel of fixed sample size rather than spatial threshold because of the Isthmus of Panama. The regional significance index is an average of the proportion of localities where the pseudo t-values (Fotheringham *et al.*, 2002) are larger than 2 for each climate predictor. The dataset representing the western part of the Old World is not included in the 2500km bandwidth for both models due to high spatial colinearity in predictor values. Similarly, we limited our analyses to bandwidths greater than 2500km because of high spatial colinearity in predictor values at lower bandwidths.

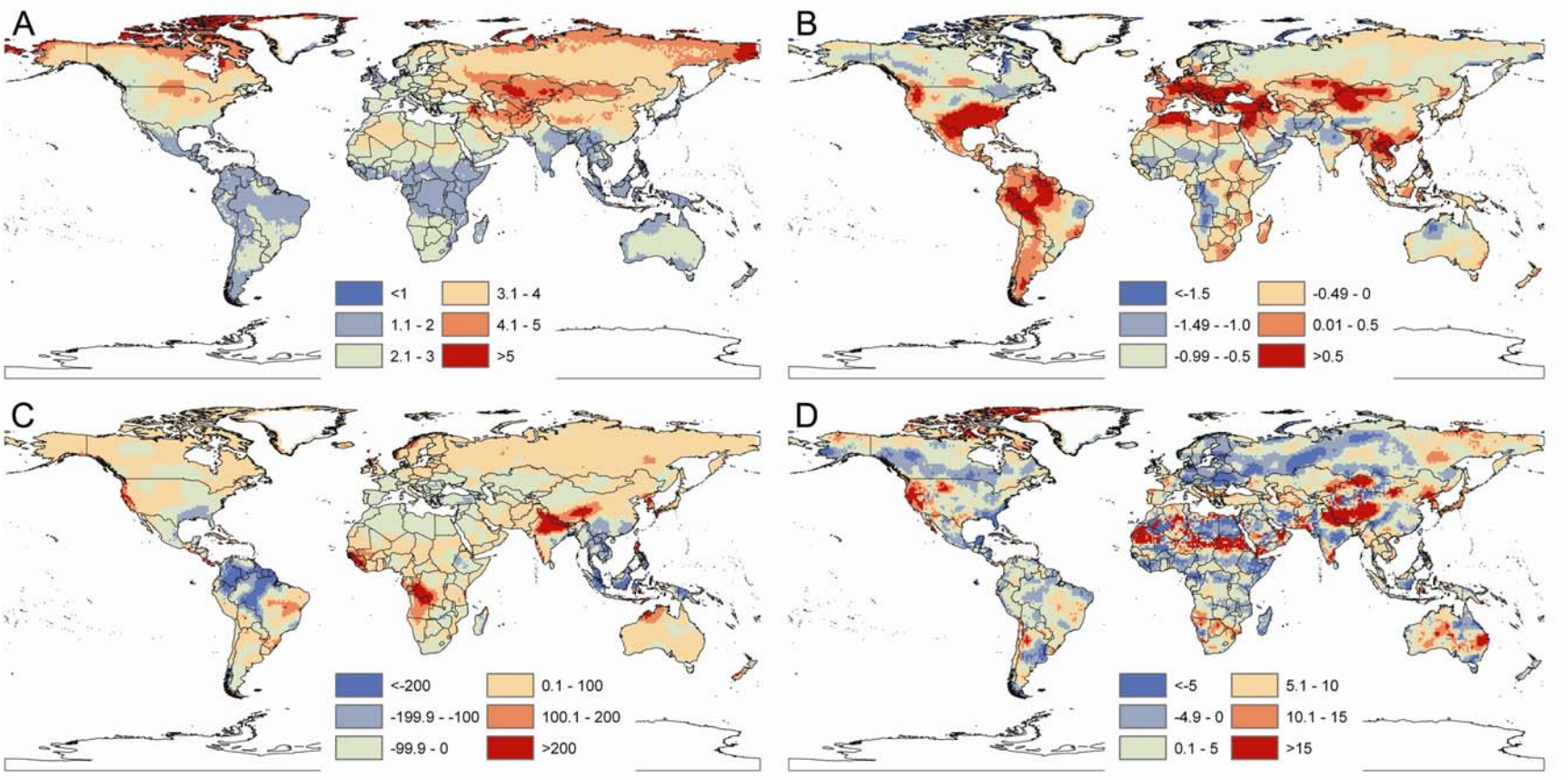

Figure S3a. Forecasted change between 1990 and 2050 in **(A)** annual mean temperature (^{o}C), **(B)** mean temperature diurnal range (^{o}C), **(C)** total annual precipitation (mm), and **(D)** precipitation seasonality (coefficient of variation). Based on interpolated data from the CCCMA 2a2 general circulation model (Hijmans *et al.*, 2005).

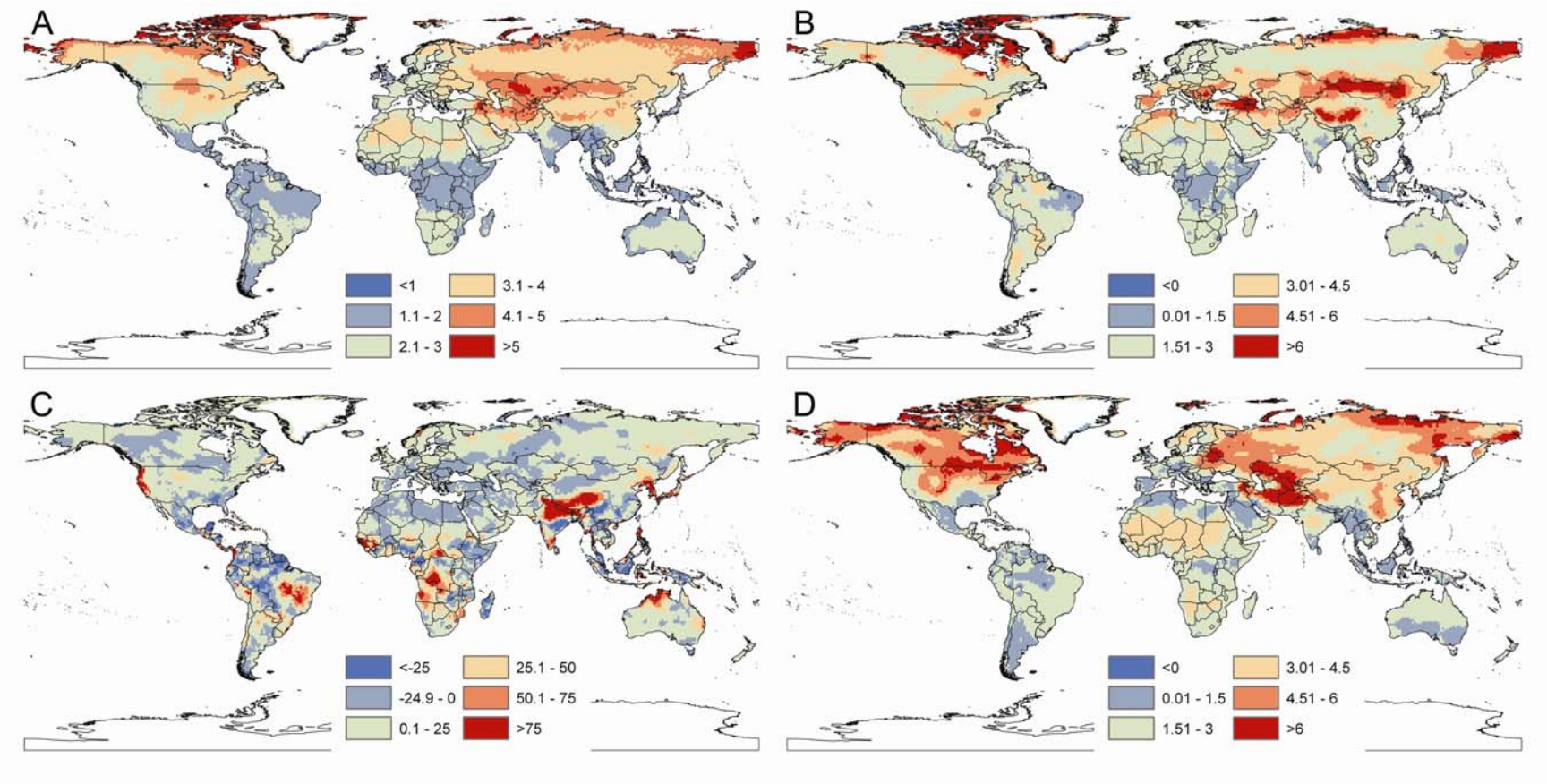

Figure S3b. Forecasted change between 1990 and 2050 in **(A)** annual mean temperature (^{o}C), **(B)** maximum temperature of the warmest month (^{o}C), **(C)** precipitation of the wettest month (mm), and **(D)** minimum temperature of the coldest month (^{o}C). Based on interpolated data from the CCCMA 2a2 general circulation model (Hijmans *et al.*, 2005).

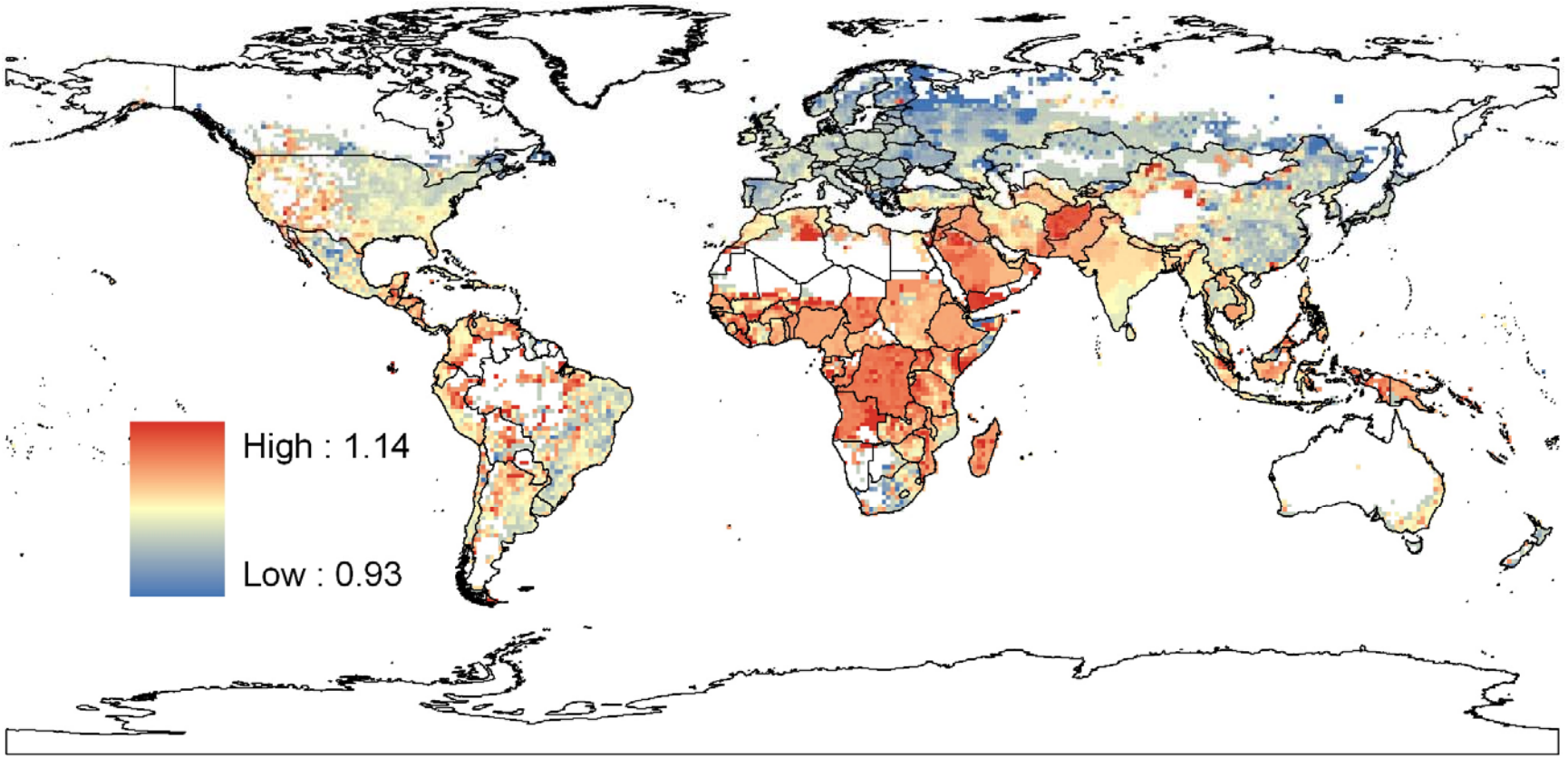

Figure S4. Human density annual growth rate between 1990 and 2015 (CIESIN, 2005)

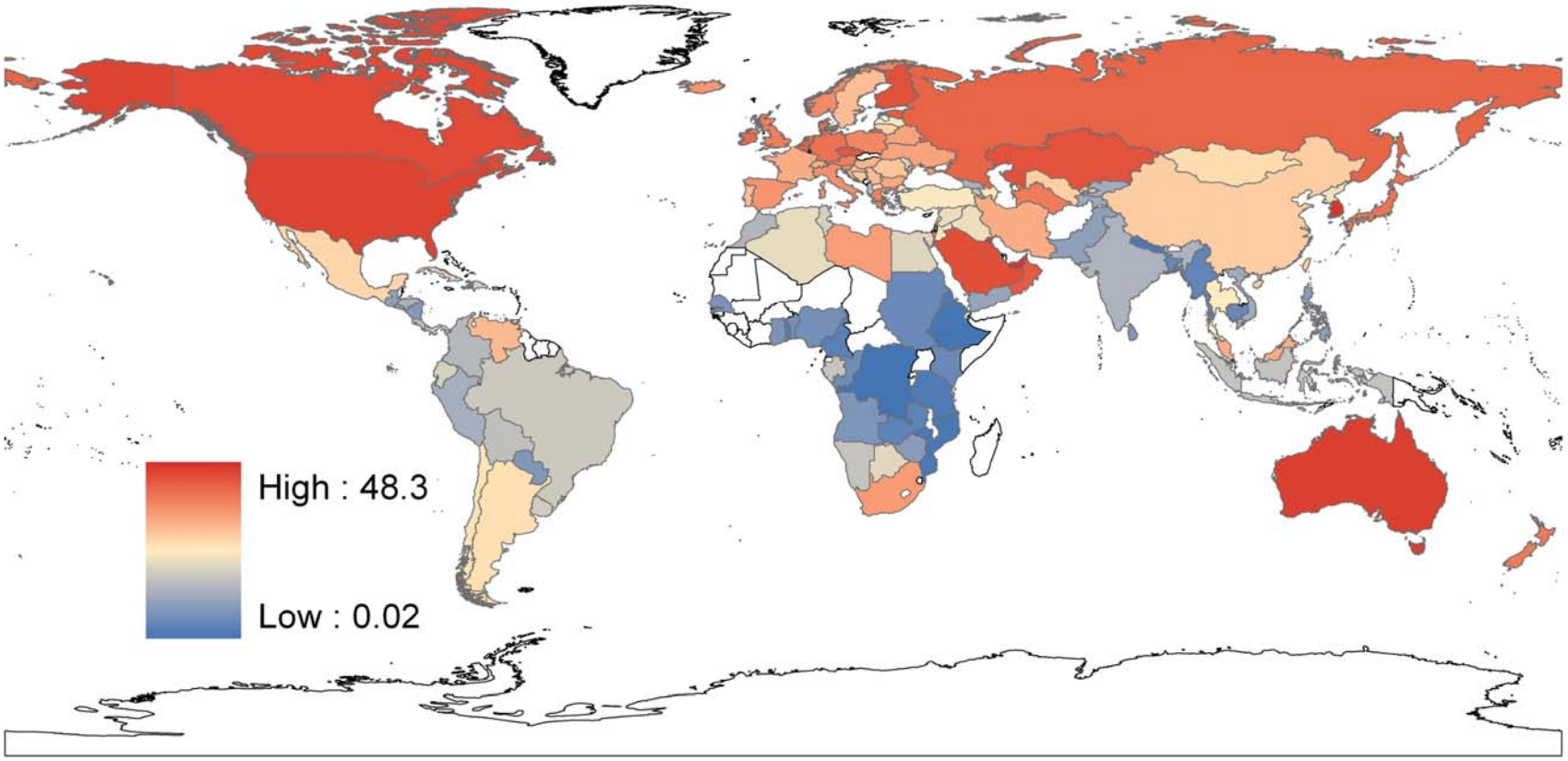

Figure S5. National average per capita CO_2 emissions based on OECD/IEA 2006 national CO_2 emissions (OECD/IEA, 2008) and UNPD 2006 national population size (UNPD, 2007). Seventy countries with UN membership but without CO_2 emission data are excluded from this analysis (displayed in white), but represented less than 2.6% of the world population in 2006.

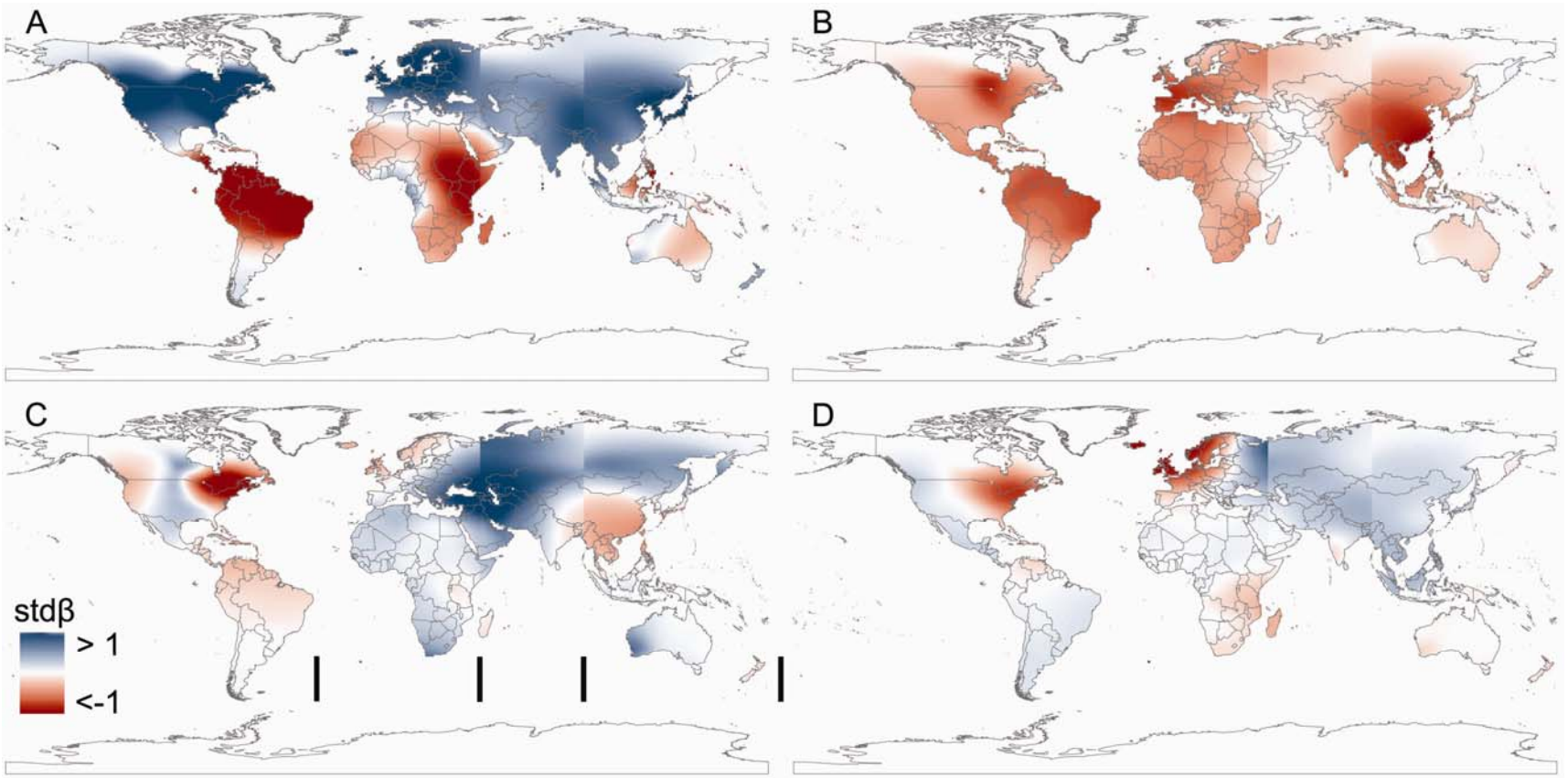

Figure S6. Standardized regression coefficients (stdβ) for **(A)** annual mean temperature (^{o}C), **(B)** mean temperature diurnal range (^{o}C), **(C)** total annual precipitation (mm), and **(D)** precipitation seasonality (coefficient of variation) from a GWR model representing 1990 human densities based on four climate predictors (average 1950-2000) and agricultural extent circa 2000 (Ramankutty *et al.*, 2008; see figure S7). The colour ramp of the legend represents stdβ values between 1 and -1 to allow direct comparison between alternative models (Fig. 2, S9, S10). The average and range of stdβ for each variable are: **(A)** 0.21: -1.5 to 4.7, **(B)** -0.31: -2.5 to 0.13, **(C)** 0.14: -1.38 to 1.17, **(D)** 0.05: -1.24 to 2.7. The black lines at the bottom of panel **(C)** represent the longitudinal breaks in the global dataset and apply to all four panels (see Methods).

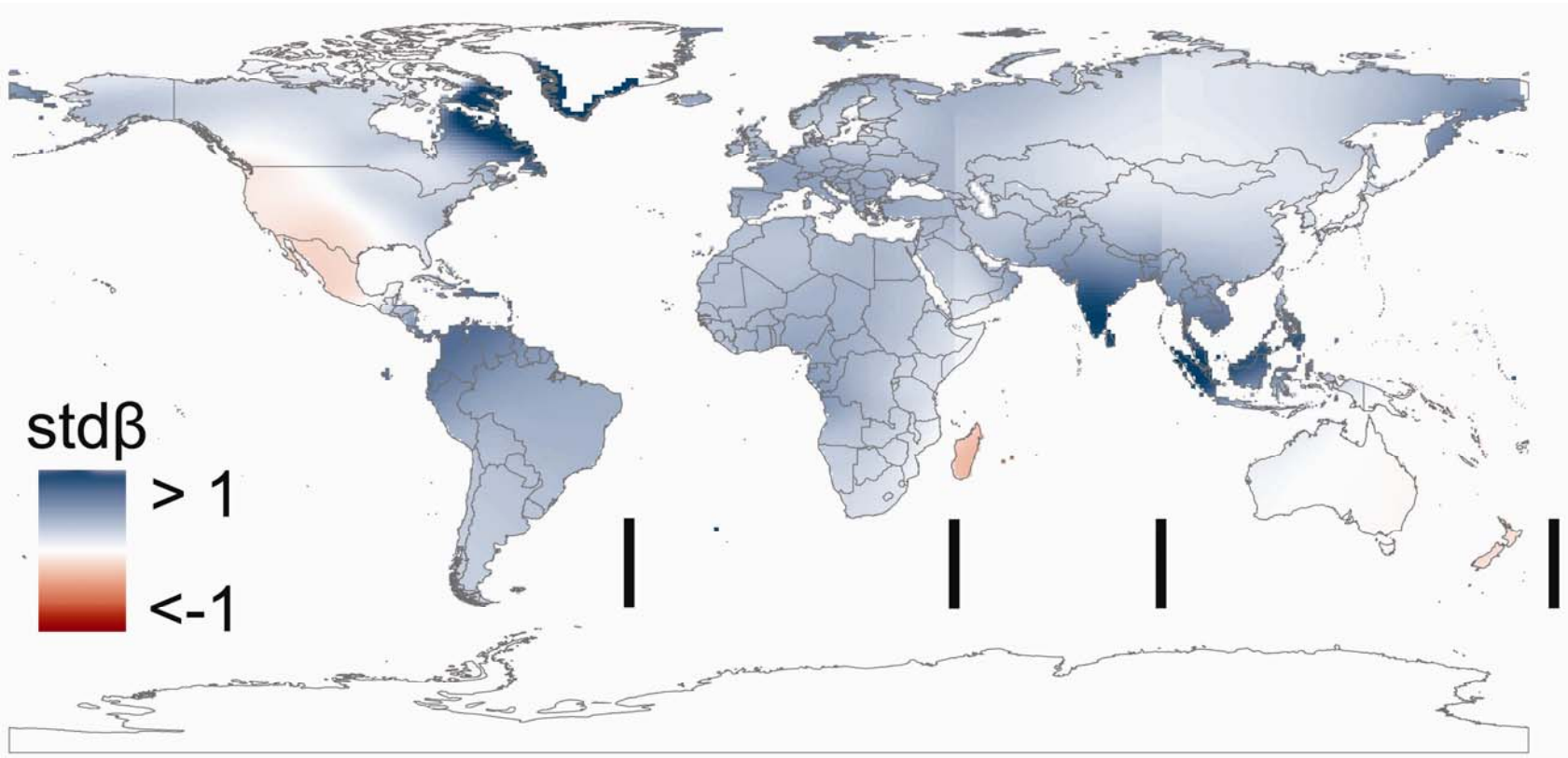

Figure S7. Standardized regression coefficients (stdβ) for agricultural extent from a GWR model representing 1990 human densities based on four climate predictors (average 1950-2000) and agricultural extent circa 2000 (Ramankutty *et al.*, 2008; see figure S6). The colour ramp of the legend represents stdβ values between 1 and -1 to allow direct comparison between alternative models (Fig. 2, S6, S8). The average and range of stdβ are: 0.27: -0.41 to 1.8. The black lines at the bottom of panel represent the longitudinal breaks in the global dataset (see Methods).

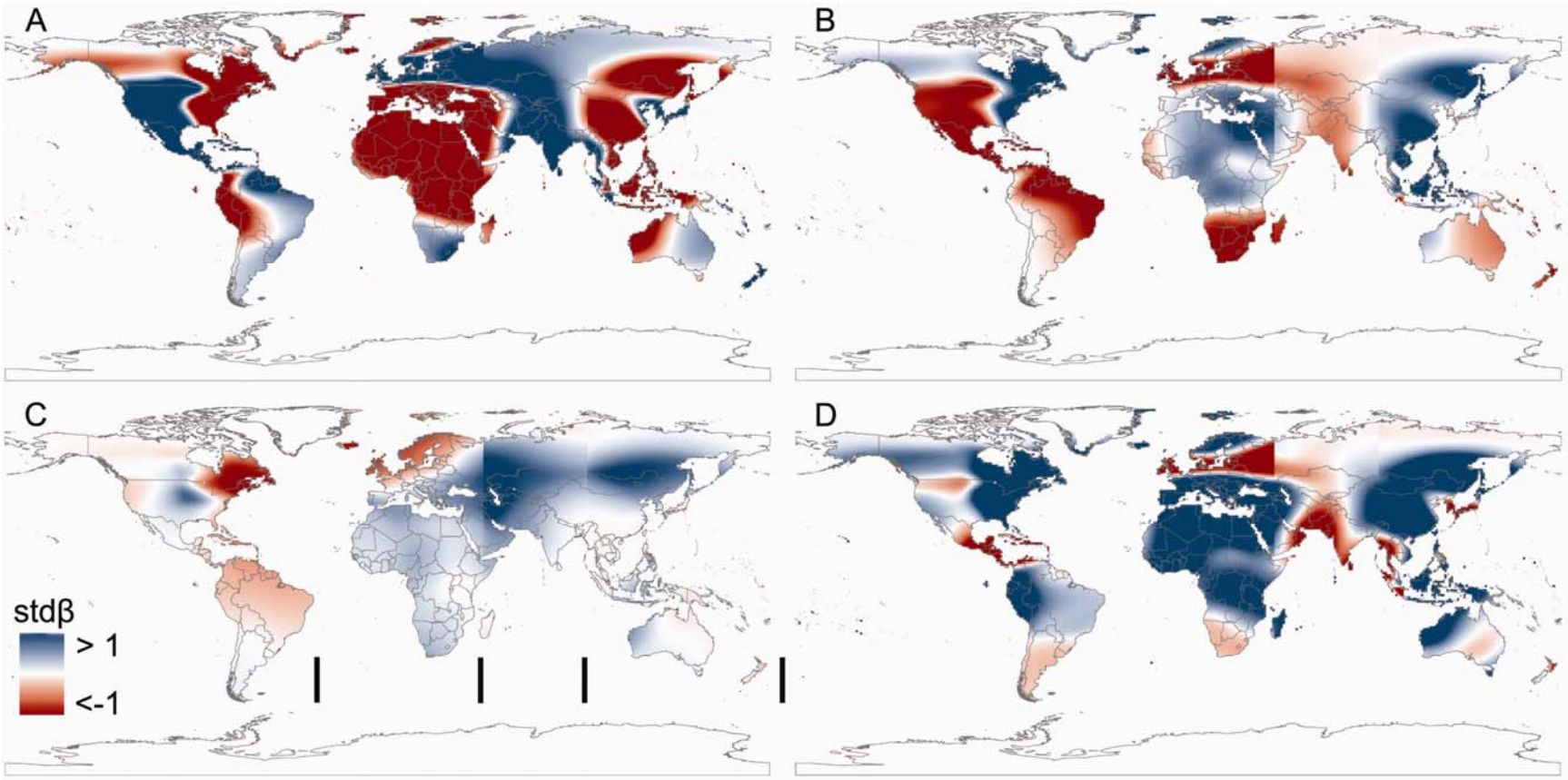

Figure S8. Standardized regression coefficients (stdβ) for **(A)** annual mean temperature (^{o}C), **(B)** minimum temperature of the coldest month (^{o}C), **(C)** precipitation of the wettest month (mm), and **(D)** maximum temperature of the warmest month (^{o}C) from a GWR model between 1990 human densities and four climate predictors (1950-2000 average). The colour ramp of the legend represents stdβ values between 1 and -1 to allow direct comparison between alternative models (Fig. 2, S6, S7). The average and range of stdβ for each variable are: **(A)** -0.35: -19.3 to 8.1, **(B)** -0.01: -8.2 to 6.8, **(C)** 0.15: -1.2 to 1.3, **(D)** 0.71: -5.3 to 19.0. The black lines at the bottom of panel **(C)** represent the longitudinal breaks in the global dataset and apply to all four panels (see Methods).

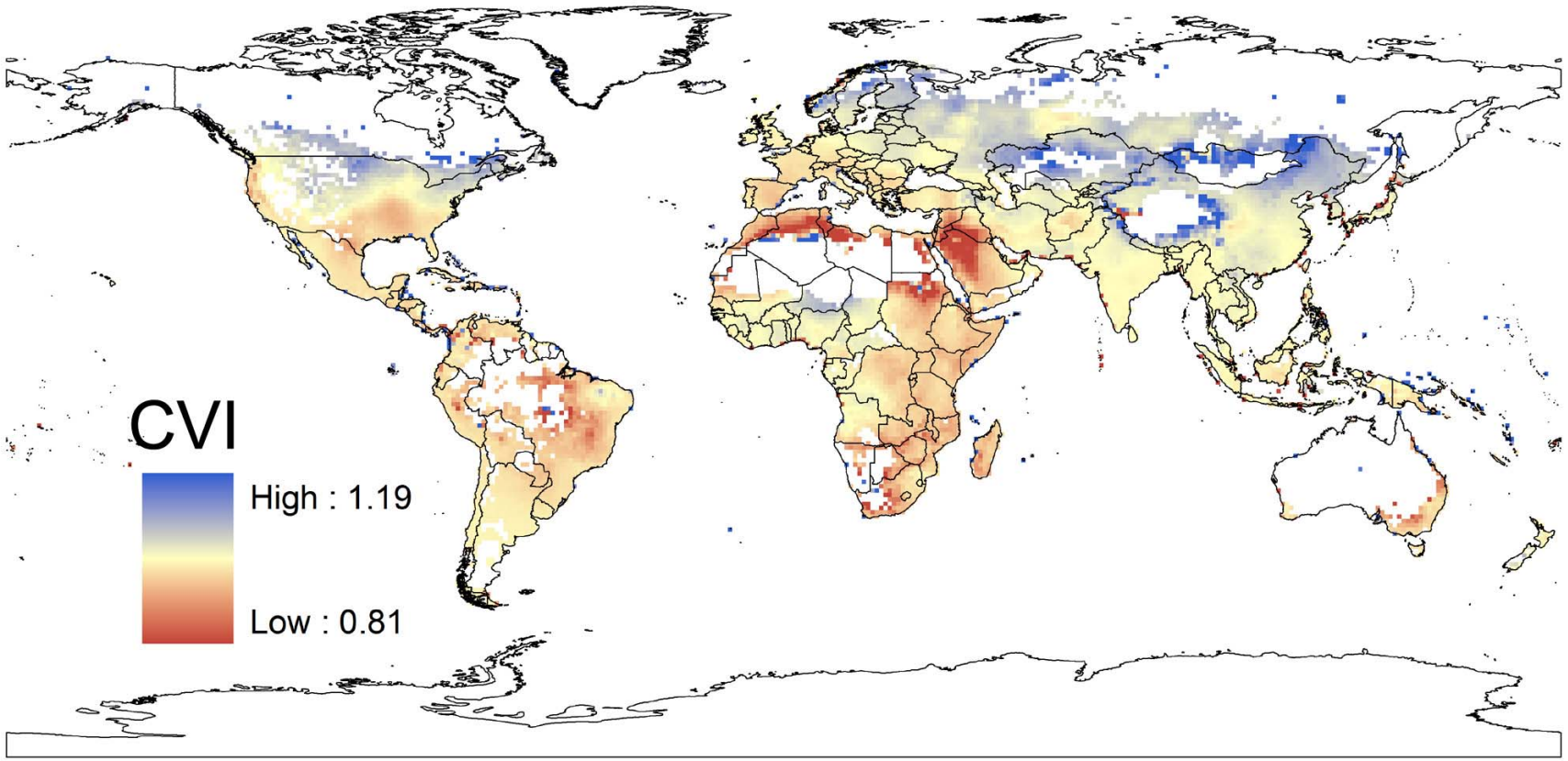

Figure S9. Climate vulnerabilities index (*CVI*) expressed as climate consistent changes in human density annual growth rate based on a GWR model between 1990 human density and four climate predictors (Fig. S8) and a 2050 climate forecast (Fig S3b). Climate consistent changes in annual growth rate less than one, indicated in red, represent high vulnerabilities while climate consistent changes in annual growth rates greater than one, indicated in blue, represent low vulnerabilities. White regions correspond to zero human density in the 1990 dataset.

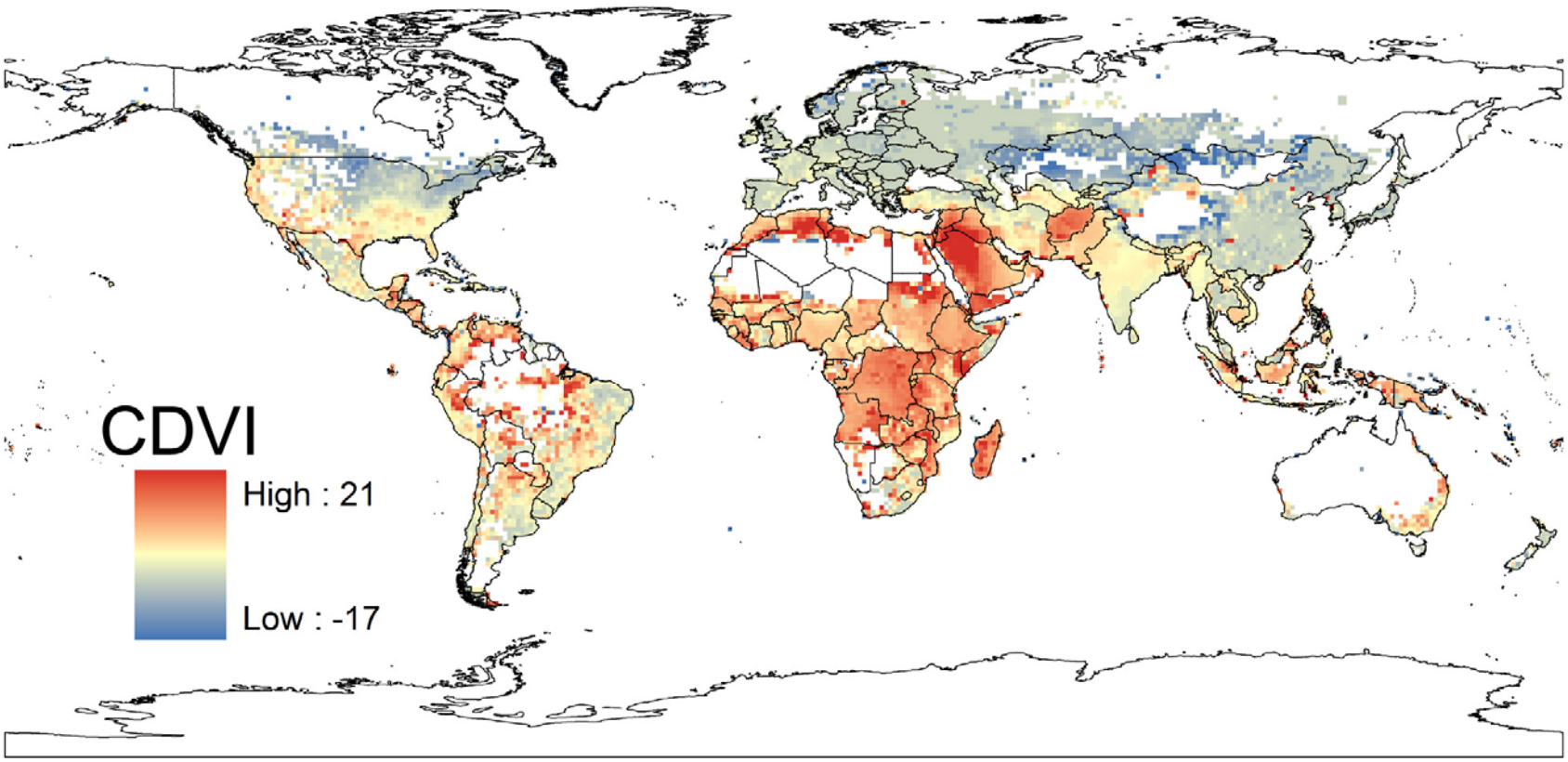

Figure S10. Global climate-demography vulnerability index (*CDVI*) estimated by subtracting climate vulnerabilities (Fig. S9) from demographic annual growth rates (Fig. S4), displayed as percentage of human density annual growth rates. Values less than one, indicated in blue, represent low stress and values greater than one, indicated in red, represent high stress. White regions correspond to zero human density values in the 1990 dataset.

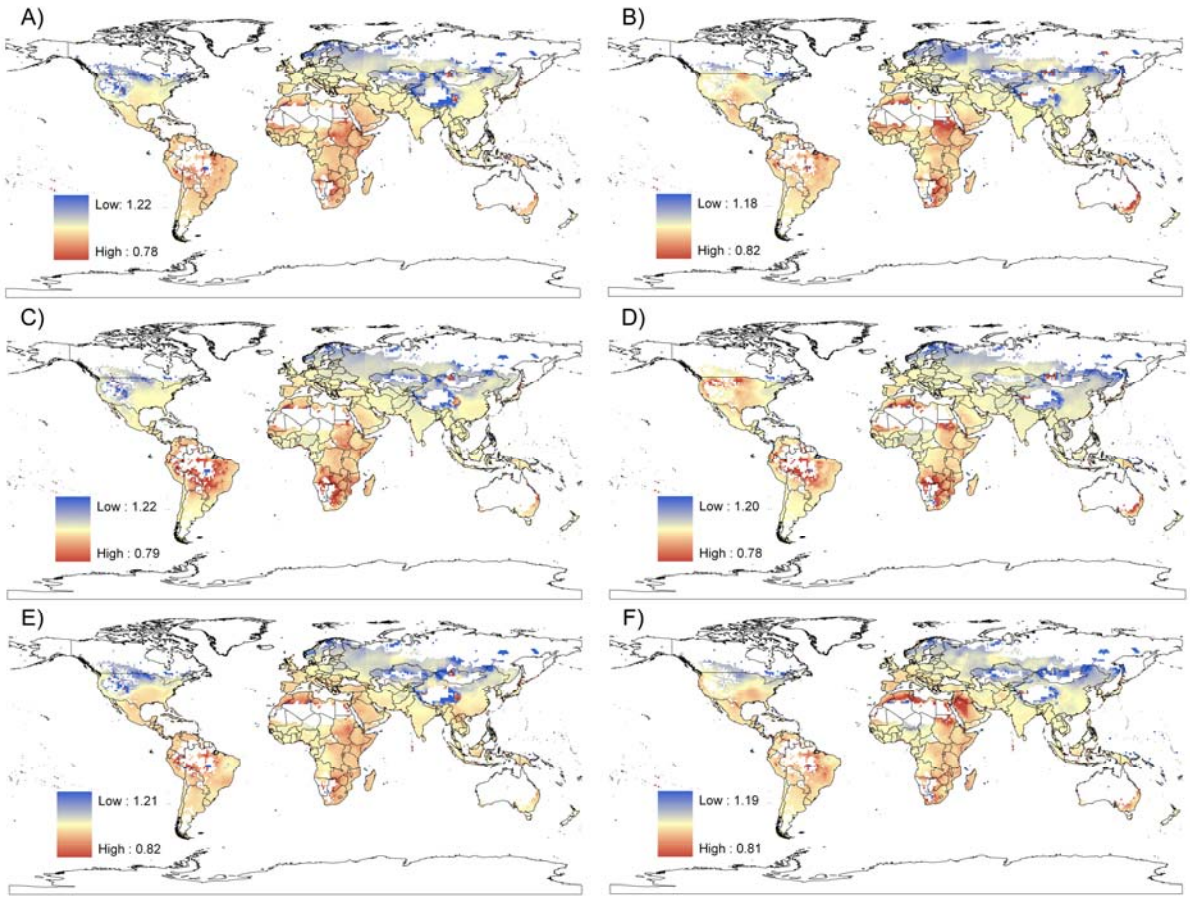

Figure S11. Climate vulnerabilities (CVI) expressed as climate consistent changes in annual growth rate based on two human-climate models (panels A, C, E represent model shown in Fig. 3, and panels B, D, F represent model shown in Fig. S8) and three general circulation models for 2050 under the A2 scenario (panel A-B: CSIRO, panel C-D: HADCM3, panel E-F: CCCMA). Human density annual growth rates less than one represent high vulnerabilities and conversely. White regions correspond to zero human density values in the 1990 dataset.

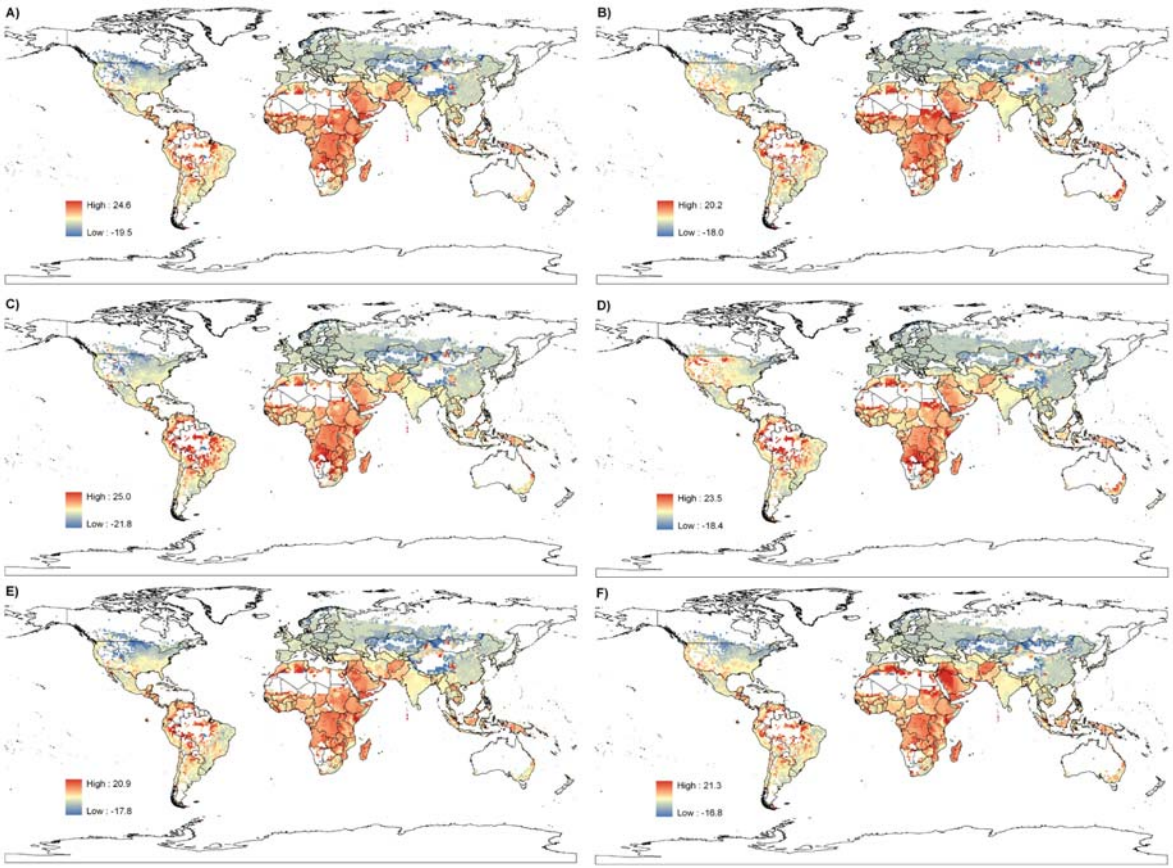

Figure S12. Global patterns of climate-demography vulnerability index (*CDVI*) for two human-climate regression models (panels A, C, E represent model shown in Fig. 3, and panels B, D, F represent model shown in Fig. S8) and three general circulation models for 2050 under the A2 scenario (panel A-B: CSIRO, panel C-D: HADCM3, panel E-F: CCCMA). Values are expressed as percentage of human density annual growth rates and positive values represent high vulnerability and conversely. White regions correspond to zero human density values in the 1990 dataset. Global average and standard deviation (in parenthesis) of *CDVI* for each model are: A) 1.09 (2.23), B) 1.33 (2.08), C) 1.34 (2.43), D) 1.53 (2.38), E) 1.03 (2.19), F) 1.24 (2.19).

REFERENCES

Center for International Earth Science Information Network (CIESIN), Columbia University; and Centro Internacional de Agricultura Tropical (CIAT). 2005. Gridded Population of the World Version 3 (GPWv3): Population Density Grids. Palisades, NY: Socioeconomic Data and Applications Center (SEDAC), Columbia University. Available at http://sedac.ciesin.columbia.edu/gpw. (downloaded on January 4th 2009).

Fotheringham, A.S., Brundson, C. & Charlton, M. (2002) *Geographically weighted regression: the analysis of spatially varying relationships*. John Wiley & Sons, Hoboken, NJ.

Hijmans, R.J., Cameron, S.E., Parra, J.L., Jones, P.G. & Jarvis, A. (2005) Very high resolution interpolated climate surfaces for global land areas. *International Journal of Climatology*, **25**, 1965-1978.

OECD/IEA (2008) CO_2 Emissions from Fuel Combustion.

Ramankutty, N., Evan, A.T., Monfreda, C. & Foley, J.A. (2008) Farming the planet: 1. Geographic distribution of global agricultural lands in the year 2000. *Global Biogeochem. Cycles*, **22**, GB1003.

UNPD (2007) UN Population Division. United Nations Environment Programme/DEWA/GRID-Geneva.